

**POSSIBLE RELICS FROM NEW PHYSICS IN THE EARLY UNIVERSE:
INFLATION, THE COSMIC MICROWAVE BACKGROUND, AND PARTICLE
DARK MATTER**

MARC KAMIONKOWSKI^b

Department of Physics, Columbia University, 538 West 120th St., New York, NY 10027 U.S.A

I review two different connections between particle theory and early-Universe cosmology: (1) Cosmic-microwave-background (CMB) tests of inflation and (2) particle dark matter. The inflationary predictions of a flat Universe and a nearly scale-invariant spectrum of primordial density perturbations will be tested precisely with forthcoming maps of the CMB temperature. A stochastic gravitational-wave background may be probed with a map of the CMB polarization. I also discuss some other uses of CMB maps. Particle theory has produced two very well-motivated candidates for the dark matter in the Universe: an axion and a supersymmetric particle. In both cases, there are a variety of experiments afoot to detect these particles. I review the properties of these dark-matter candidates and these detection techniques.

1 Introduction

In recent decades, particle theorists and cosmologists have joined forces in an effort to uncover evidence for new physics beyond the standard model while simultaneously trying to reconstruct the events that occurred during the first second after the big bang. At first, this endeavor yielded a plethora of ideas. Although many of these early hypotheses have fallen by the wayside, several have remained intact, become increasingly attractive, and are currently under experimental scrutiny. The purpose of these lectures is to review what I believe to be two of the currently most compelling connections between particle physics and early-Universe cosmology: Cosmic microwave background (CMB) tests of inflation and the particle solution to the dark-matter problem.

1.1 *Inflation and the Cosmic Microwave Background*

Despite its major triumphs (the expansion, nucleosynthesis, and the cosmic microwave background), the big-bang theory for the origin of the Universe leaves several questions unanswered. Chief amongst these is the horizon problem: When cosmic microwave background (CMB) photons last scattered, the age of the Universe was roughly 100,000 years, much smaller than its current age of roughly 10 billion years. After taking into account the expansion of the Universe, one finds that the angle subtended by a causally connected region at the surface of last scatter is roughly 1° . However, there are 40,000 square degrees on the surface of the sky. Therefore, when we look at the CMB over the entire sky, we are looking at 40,000 causally disconnected regions of the Universe. But quite remarkably, each has the same temperature to roughly one part in 10^5 !

The most satisfying (only?) explanation for this is slow-roll inflation [1], a period of accelerated expansion in the early Universe driven by the vacuum energy most likely associated with a symmetric phase of a GUT Higgs field (or perhaps Planck-scale physics or Peccei-Quinn symmetry breaking). Although the physics responsible for inflation is still not well understood,

^aTo appear in *The Early and Future Universe*, proceedings of the CCAST workshop, Beijing, China, June 22–27, 1998, edited by Minghan Ye (Gordon and Breach Publishers).

^bkamion@phys.columbia.edu

inflation generically predicts (1) a flat Universe; (2) that primordial adiabatic (i.e., curvature) perturbations are responsible for the large-scale structure (LSS) in the Universe today [2]; and (3) a stochastic gravity-wave background [3]. More precisely, inflation predicts a spectrum $P_s = A_s k^{n_s}$ (with n_s near unity) of primordial density (scalar metric) perturbations, and a stochastic gravity-wave background (tensor metric perturbations) with spectrum $P_t = A_t \propto k^{n_t}$ (with n_t small compared with unity). (4) Inflation further uniquely predicts specific relations between the “inflationary observables,” the amplitudes A_s and A_t and spectral indices n_s and n_t of the scalar and tensor perturbations [4]. The amplitude of the gravity-wave background is proportional to the height of the inflaton potential, and the spectral indices depend on the shape of the inflaton potential. Therefore, determination of these parameters would illuminate the physics responsible for inflation.

Until recently, none of these predictions could really be tested. Measured values for the density of the Universe span almost an order of magnitude. Furthermore, most do not probe the possible contribution of a cosmological constant (or some other diffuse matter component), so they do not address the geometry of the Universe. The only observable effects of a stochastic gravity-wave background are in the CMB. COBE observations do in fact provide an upper limit to the tensor amplitude, and therefore an inflaton-potential height near the GUT scale. However, there is no way to disentangle the scalar and tensor contributions to the COBE anisotropy.

It has recently become increasingly likely that adiabatic perturbations are responsible for the origin of structure. Before COBE, there were numerous plausible models for structure formation: e.g., isocurvature perturbations both with and without cold dark matter, late-time or slow phase transitions, topological defects (cosmic strings or textures), superconducting cosmic strings, explosive or seed models, a “loitering” Universe, etc. However, the amplitude of the COBE anisotropy makes all these alternative models unlikely. With adiabatic perturbations, hotter regions at the surface of last scatter are embedded in deeper potential wells, so the reddening due to the the gravitational redshift of the photons from these regions partially cancels the higher intrinsic temperatures. Thus, other models will generically produce more anisotropy for the same density perturbation. When normalized to the density fluctuations indicated by galaxy surveys, alternative models thus generically produce a larger temperature fluctuation than that measured by COBE [5]. In the past year, some leading proponents of topological defects, the leading alternative, have conceded that these models have difficulty accounting for the origin of large-scale structure [6].

We are now entering an exciting new era, driven by new theoretical ideas and developments in detector technology, in which the predictions of inflation will be tested with unprecedented precision. It is even conceivable that early in the next century, we will move from verification to direct investigation of the high-energy physics responsible for inflation.

1.2 Dark Matter and New Particles

Another of the grand cosmic mysteries today is the nature of the dark matter. Almost all astronomers will agree that most of the mass in the Universe is nonluminous. Dynamics of clusters of galaxies suggest a universal nonrelativistic-matter density of $\Omega_0 \simeq 0.1 - 0.3$. If the luminous matter were all there was, the duration of the epoch of structure formation would be very short, thereby requiring (in almost all theories of structure formation) fluctuations in the CMB which would be larger than those observed. These considerations imply $\Omega_0 \gtrsim 0.3$ [7]. Second, if the current value of Ω_0 is of order unity today, then at the Planck time it must have been 1 ± 10^{-60} leading us to believe that Ω_0 is precisely unity for aesthetic reasons. And of course, inflation, must set Ω , the *total* density (including a cosmological constant), to unity.

However, the most robust observational evidence for the existence of dark matter involves galactic dynamics. There is simply not enough luminous matter ($\Omega_{\text{lum}} \lesssim 0.01$) observed in spiral

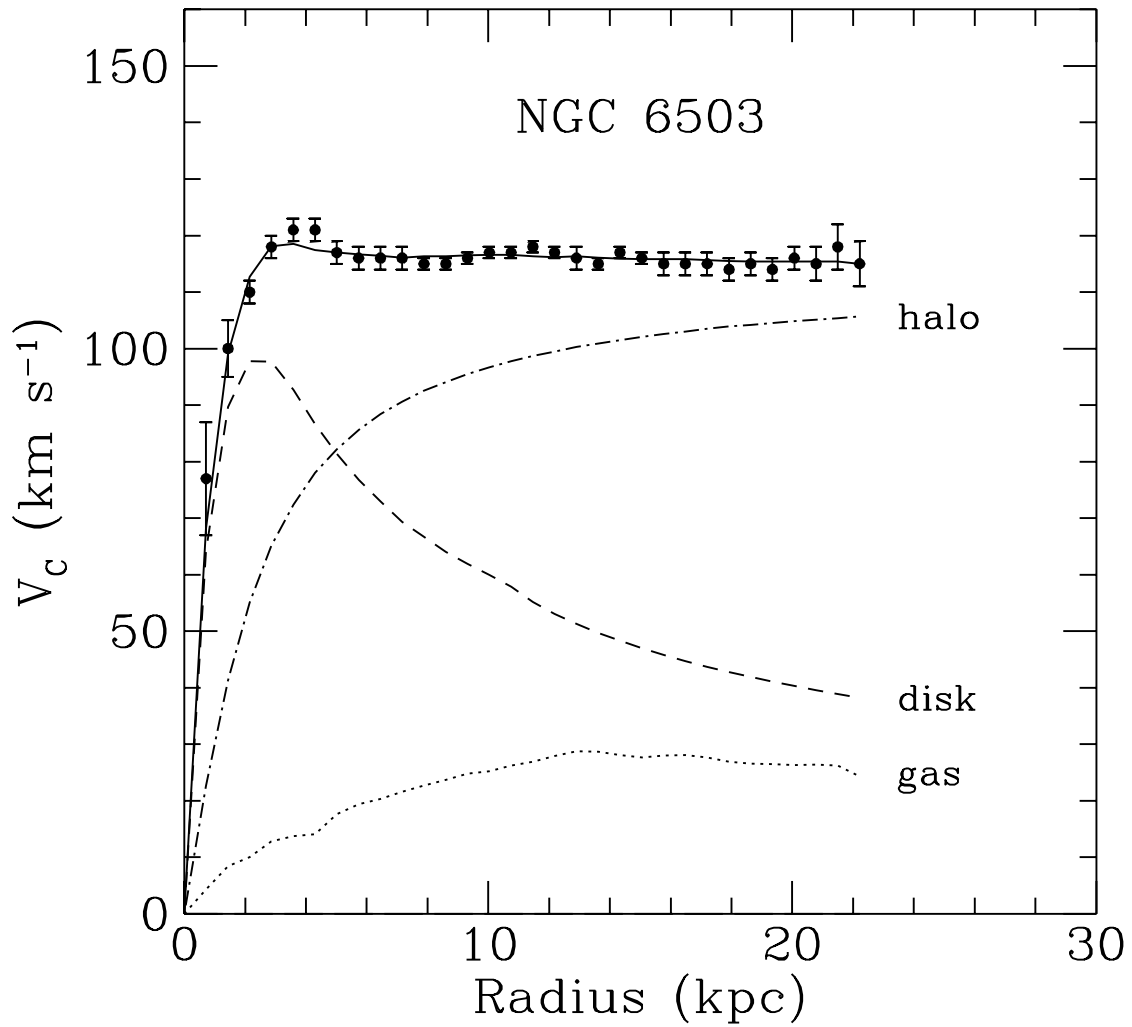


Figure 1: Rotation curve for the spiral galaxy NGC6503. The points are the measured circular rotation velocities as a function of distance from the center of the galaxy. The dashed and dotted curves are the contribution to the rotational velocity due to the observed disk and gas, respectively, and the dot-dash curve is the contribution from the dark halo.

galaxies to account for their observed rotation curves (for example, that for NGC6503 shown in Fig. 1 [8]). Newton's laws imply galactic dark halos with masses that contribute $\Omega_{\text{halo}} \gtrsim 0.1$.

On the other hand, big-bang nucleosynthesis suggests that the baryon density is $\Omega_b \lesssim 0.1$ [9], too small to account for the dark matter in the Universe. Although a neutrino species of mass $\mathcal{O}(30\text{ eV})$ could provide the right dark-matter density, N-body simulations of structure formation in a neutrino-dominated Universe do a poor job of reproducing the observed structure [10]. Furthermore, it is difficult to see (essentially from the Pauli principle) how such a neutrino could make up the dark matter in the halos of galaxies [11]. It appears likely then, that some nonbaryonic, nonrelativistic matter is required.

The two leading candidates from particle theory are the axion [12], which arises in the Peccei-Quinn solution to the strong- CP problem, and a weakly-interacting massive particle (WIMP), which may arise in supersymmetric (or other) extensions of the standard model [13]. As discussed below, there are good reasons to believe that if the Peccei-Quinn mechanism is responsible for preserving CP in the strong interactions, then the axion is the dark matter. Similarly, there are also excellent reasons to expect that if low-energy supersymmetry exists in Nature, then the dark matter should be composed of the lightest superpartner. The study of these ideas are no longer exclusively the domain of theorists: there are now a number of experiments aimed at discovery of axions and WIMPs. If axions populate the Galactic halo, they can be converted to photons in resonant cavities immersed in strong magnetic fields. An experiment to search for axions in this fashion is currently being carried out. If WIMPs populate the halo, they can be detected either directly in low-background laboratory detectors or indirectly via observation of energetic neutrinos from WIMPs which have accumulated and then annihilated in the Sun and/or Earth.

1.3 Outline

One of the purposes of these lectures is to review how forthcoming CMB experiments will test several of the predictions of inflation. I will not have time to provide a real review of inflation. For more details on inflation (as well as the standard cosmological model), see the books by Kolb and Turner [14] and/or Peebles [15], or the lectures in these proceedings by Steinhardt. Here, I will first review the predictions of inflation for density perturbations and gravity waves. I will then discuss how CMB temperature anisotropies will test the inflationary predictions of a flat Universe and a primordial spectrum of density perturbations. I review how a CMB polarization map may be used to isolate the gravity waves and briefly review how detection of these tensor modes may be used to learn about the physics responsible for inflation.

Although my focus here is on CMB tests of inflation, the CMB may also be useful for addressing some other issues in cosmology that may be of only tangential relevance to inflation, and I briefly review a few of those here. I discuss some recent work on secondary anisotropies at smaller angular scales, and how these may be used to probe the epoch at which objects first underwent gravitational collapse in the Universe. I then briefly mention a few other possibilities.

In the Section on dark matter, I first show how the observed dynamics of the Milky Way indicate a local dark-matter density of $\rho_0 \simeq 0.4\text{ GeV cm}^{-3}$. I then review the arguments for axion and WIMP dark matter and the methods of detection. However, there is no way I can do this very active field of research justice in such a short space. Readers with further interest in WIMPs should see the review article by Jungman, Griest and me [13]. The first four Sections of that article are meant to provide a general review of dark and supersymmetry, and the idea of WIMP dark matter. The remainder of that article provides technical details required by those interested in actively pursuing research on the topic. There are also several excellent axion reviews [12] and the recent book by Raffelt [16].

2 The Cosmic Microwave Background and Inflation

2.1 Inflationary Observables

Inflation occurs when the energy density of the Universe is dominated by the vacuum energy $V(\phi)$ associated with some scalar field ϕ (the “inflaton”). During this time, the quantum fluctuations in ϕ produce classical scalar perturbations, and quantum fluctuations in the spacetime metric produce gravitational waves. If the inflaton potential $V(\phi)$ is given in units of m_{Pl}^4 , and the inflaton ϕ is in units of m_{Pl} , then the scalar and tensor spectral indices are

$$\begin{aligned} 1 - n_s &= \frac{1}{8\pi} \left(\frac{V'}{V} \right)^2 - \frac{1}{4\pi} \left(\frac{V'}{V} \right)', \\ n_t &= -\frac{1}{8\pi} \left(\frac{V'}{V} \right)^2. \end{aligned} \quad (1)$$

The amplitudes can be fixed by their contribution to C_2^{TT} , the quadrupole moment of the CMB temperature,

$$\begin{aligned} \mathcal{S} &\equiv 6C_2^{\text{TT,scalar}} = 33.2 [V^3/(V')^2], \\ \mathcal{T} &\equiv 6C_2^{\text{TT,tensor}} = 9.2V. \end{aligned} \quad (2)$$

For the slow-roll conditions to be satisfied, we must have

$$(1/16\pi)(V'/V)^2 \ll 1, \quad (3)$$

$$(1/8\pi)(V''/V) \ll 1, \quad (4)$$

which guarantee that inflation lasts long enough to make the Universe flat and to solve the horizon problem.

When combined with COBE results, current degree-scale–anisotropy and large-scale-structure observations suggest that \mathcal{T}/\mathcal{S} is less than order unity in inflationary models, which restricts $V \lesssim 5 \times 10^{-12}$. Barring strange coincidences, the COBE spectral index and relations above suggest that if slow-roll inflation is right, then the scalar and tensor spectra must both be nearly scale invariant ($n_s \simeq 1$ and $n_t \simeq 0$).

2.2 Temperature Anisotropies

The primary goal of CMB experiments that map the temperature as a function of position on the sky is recovery of the temperature autocorrelation function or angular power spectrum of the CMB. The fractional temperature perturbation $\Delta T(\hat{\mathbf{n}})/T$ in a given direction $\hat{\mathbf{n}}$ can be expanded in spherical harmonics,

$$\frac{\Delta T(\hat{\mathbf{n}})}{T} = \sum_{lm} a_{(lm)}^{\text{T}} Y_{(lm)}(\hat{\mathbf{n}}), \quad \text{with} \quad a_{(lm)}^{\text{T}} = \int d\hat{\mathbf{n}} Y_{(lm)}^*(\hat{\mathbf{n}}) \frac{\Delta T(\hat{\mathbf{n}})}{T}. \quad (5)$$

Statistical isotropy and homogeneity of the Universe imply that these coefficients have expectation values $\langle (a_{(lm)}^{\text{T}})^* a_{(l'm')}^{\text{T}} \rangle = C_l^{\text{TT}} \delta_{ll'} \delta_{mm'}$ when averaged over the sky. Roughly speaking, the multipole moments C_l^{TT} measure the mean-square temperature difference between two points separated by an angle $(\theta/1^\circ) \sim 200/l$.

Predictions for the C_l 's can be made given a theory for structure formation and the values of several cosmological parameters: the total density Ω in units of the critical density, the cosmological-constant Λ in units of the critical density, the Hubble constant h in units of $100 \text{ km sec}^{-1} \text{ Mpc}^{-1}$, and the baryon density Ω_b in units of the critical density. Fig. 2 shows predictions for models with primordial adiabatic perturbations. The wriggles come from oscillations

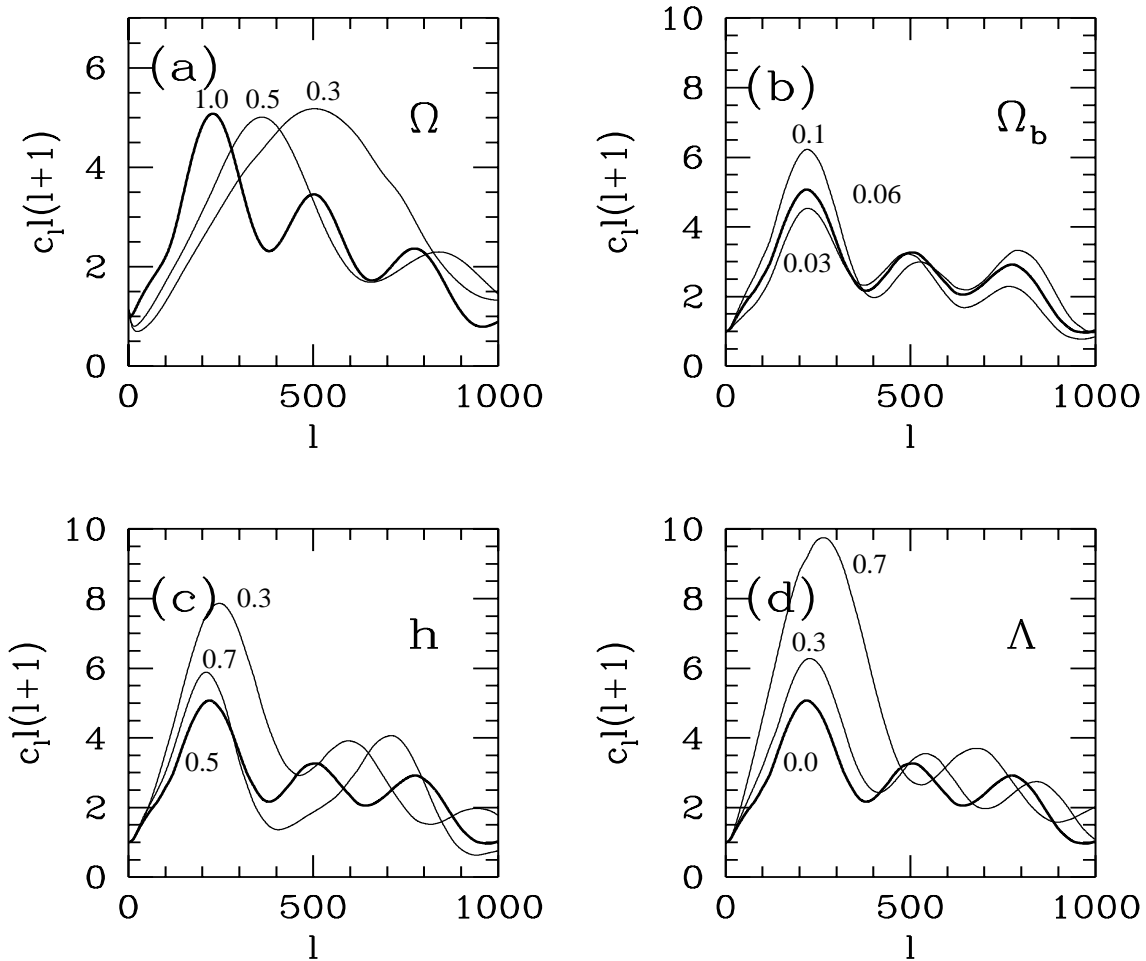


Figure 2: Theoretical predictions for CMB spectra as a function of multipole moment l for models with primordial adiabatic perturbations. In each case, the heavy curve is that for the canonical standard-CDM values, a total density $\Omega = 1$, cosmological constant $\Lambda = 0$, baryon density $\Omega_b = 0.06$, and Hubble parameter $h = 0.5$. Each graph shows the effect of variation of one of these parameters. In (d), $\Omega_0 + \Lambda = 1$.

in the photon-baryon fluid at the surface of last scatter. Each panel shows the effect of independent variation of one of the cosmological parameters. As illustrated, the height, width, and spacing of the acoustic peaks in the angular spectrum depend on these (and other) cosmological parameters.

These small-angle CMB anisotropies can be used to determine the geometry of the Universe [7]. The angle subtended by the horizon at the surface of last scatter is $\theta_H \sim \Omega^{1/2} 1^\circ$, and the peaks in the CMB spectrum are due to causal processes at the surface of last scatter. Therefore, the angles (or values of l) at which the peaks occur determine the geometry of the Universe. This is illustrated in Fig. 2(a) where the CMB spectra for several values of Ω are shown. As illustrated in the other panels, the angular position of the first peak is relatively insensitive to the values of other undetermined (or still imprecisely determined) cosmological parameters such as the baryon density, the Hubble constant, and the cosmological constant (as well as several others not shown such as the spectral indices and amplitudes of the scalar and tensor spectra and the ionization history of the Universe). Therefore, determination of the location of this first acoustic peak should provide a robust measure of the geometry of the Universe.

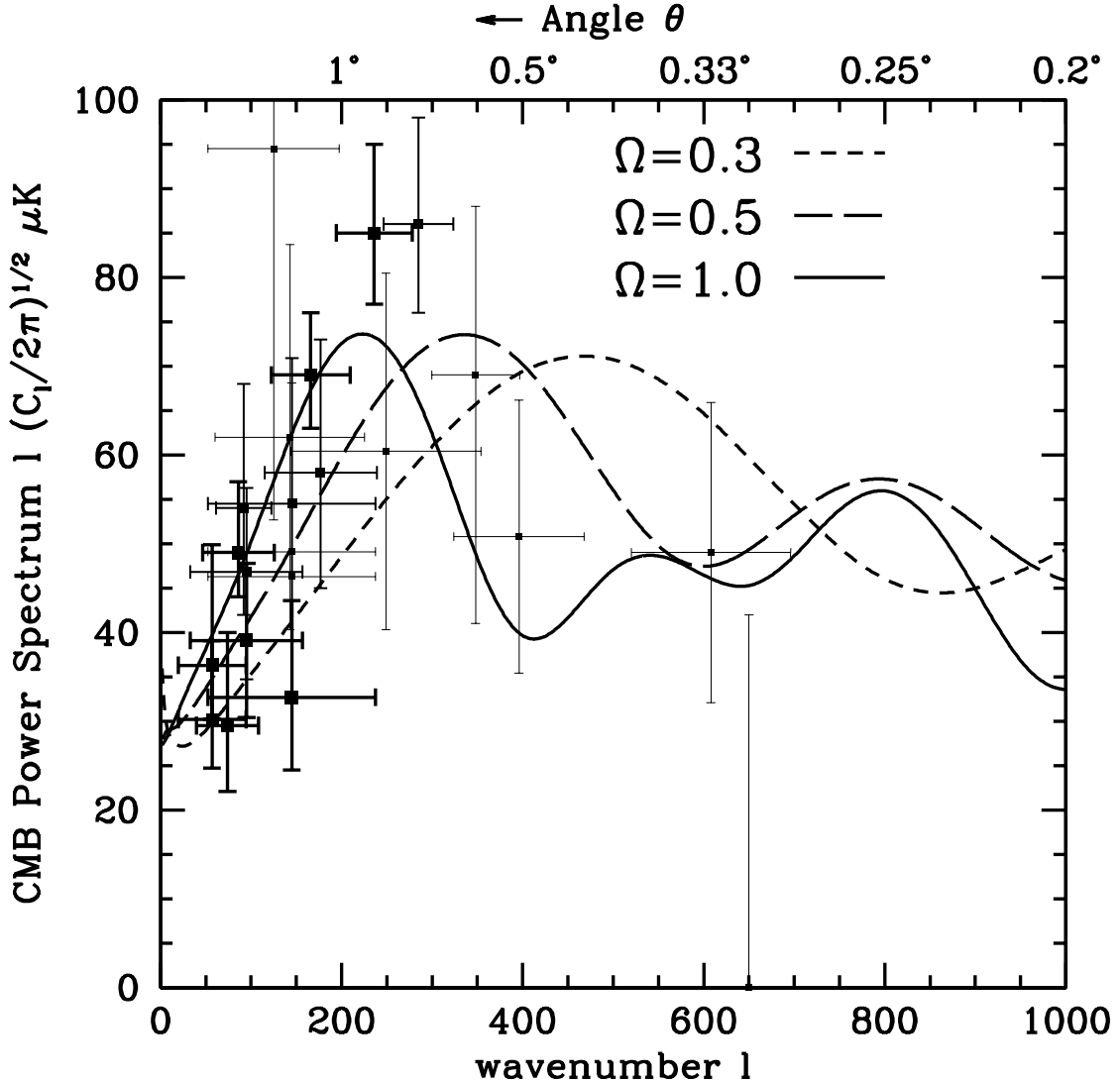


Figure 3: Current CMB data (from Ref. [17]).

Fig. 3 shows data from current ground-based and balloon-borne experiments. By fitting the theoretical curves to these points, several groups find that the best fit to the data is found with a total density $\Omega \simeq 1.0$ [18]. However, visual inspection of the data points in Fig. 3 clearly indicate that this current determination of the geometry cannot be robust.

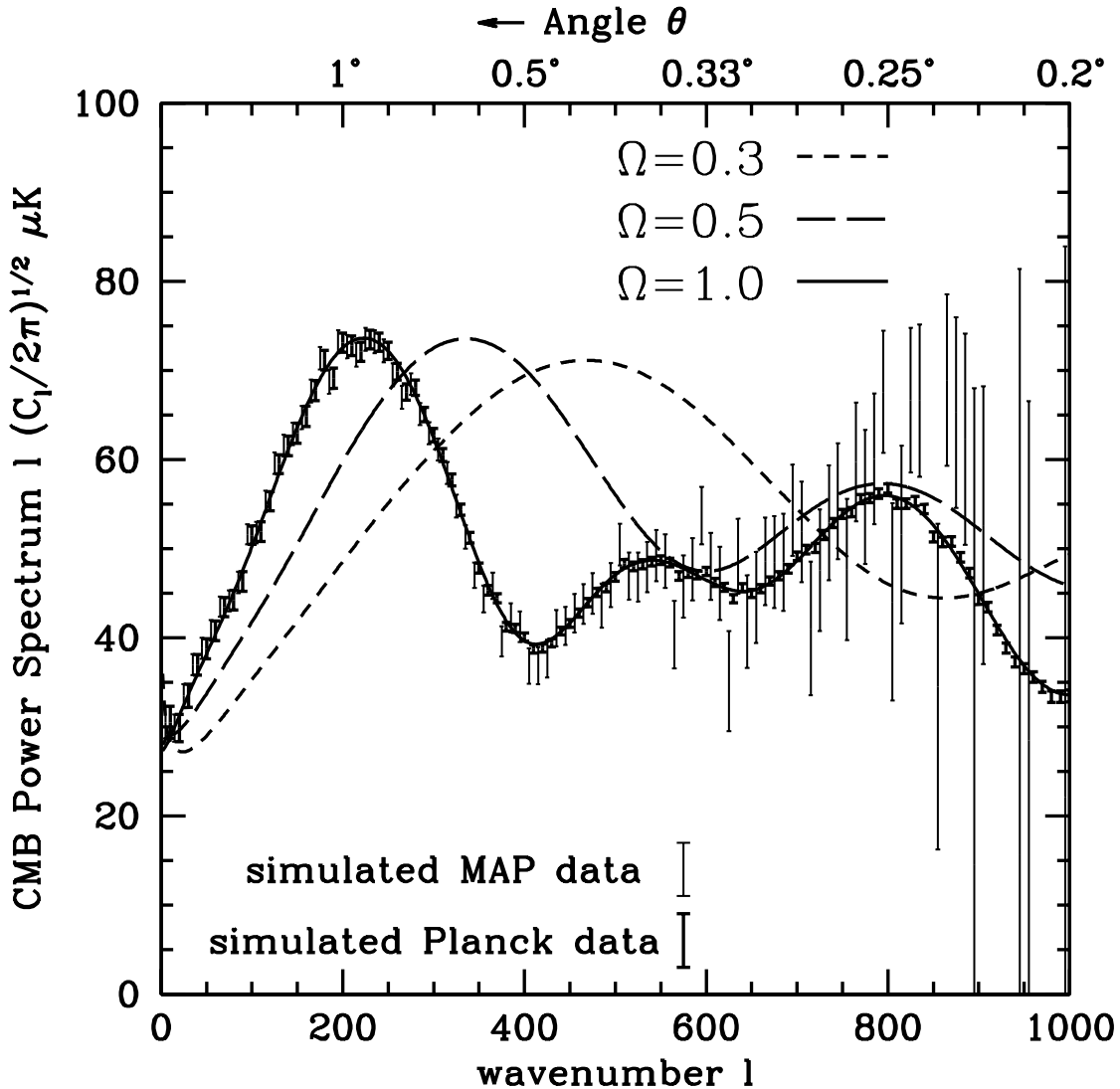


Figure 4: Simulated MAP and Planck data (from Ref. [17]).

In the near future, the precision with which this determination can be made will be improved dramatically. NASA has recently approved the flight of a satellite mission, the Microwave Anisotropy Probe (MAP) [19] in the year 2000 to carry out these measurements, and the European Space Agency (ESA) has approved the flight of a subsequent more precise experiment, the Planck Surveyor [20]. Fig. 4 shows simulated data from MAP and Planck. The heavier points with smaller error bars are those we might expect from Planck and the lighter points with larger error bars are those anticipated for MAP. Even without any sophisticated analysis, it is clear from Fig. 4 that data from either of these experiments will be able to locate the first acoustic peak sufficiently well to discriminate between a flat Universe ($\Omega = 1$) and an open Universe with $\Omega \simeq 0.3 - 0.5$.

By doing what essentially boils down to a calculation of the covariance matrix for such

simulated data, it can be shown that these satellite missions may potentially determine Ω to better than 10% *after* marginalizing over all other undetermined parameters (we considered 7 more parameters in addition to the 4 shown in Fig. 2), and better than 1% if the other parameters can be fixed by independent observations or assumption [21]. This would be far more accurate than any traditional determinations of the geometry.

It can similarly be shown that the CMB should provide values for the cosmological constant and baryon density far more precise than those from traditional observations [22,23]. If there is more nonrelativistic matter in the Universe than baryons can account for—as suggested by current observations—it will become increasingly clear with future CMB measurements.

Although these initial forecasts relied on the assumptions that adiabatic perturbations were responsible for structure formation and that reionization would not erase CMB anisotropies, these assumptions have become increasingly justifiable in the past few years. As discussed above, the leading alternative theories for structure formation now appear to be in trouble, and recent detections of CMB anisotropy at degree angular separations show that the effects of reionization are small.

The predictions of a nearly scale-free spectrum of primordial adiabatic perturbations will also be further tested with measurements of small-angle CMB anisotropies. The existence and structure of the acoustic peaks shown in Fig. 2 will provide an unmistakable signature of adiabatic perturbations [24] and the spectral index n_s can be determined from fitting the theoretical curves to the data in the same way that the density, cosmological constant, baryon density, and Hubble constant are also fit [22].

Temperature anisotropies produced by a stochastic gravity-wave background would affect the shape of the angular CMB spectrum, but there is no way to disentangle the scalar and tensor contributions to the CMB anisotropy in a model-independent way. Unless the tensor signal is large, the cosmic variance from the dominant scalar modes will provide an irreducible limit to the sensitivity of a temperature map to a tensor signal [22].

2.3 CMB Polarization and Gravitational Waves

Although a CMB temperature map cannot unambiguously distinguish between the density-perturbation and gravity-wave contributions to the CMB, the two can be decomposed in a model-independent fashion with a map of the CMB polarization [25,26,27]. Suppose we measure the linear-polarization “vector” $\vec{P}(\hat{\mathbf{n}})$ at every point $\hat{\mathbf{n}}$ on the sky. Such a vector field can be written as the gradient of a scalar function A plus the curl of a vector field \vec{B} : $\vec{P}(\hat{\mathbf{n}}) = \vec{\nabla}A + \vec{\nabla} \times \vec{B}$. The gradient (i.e., curl-free) and curl components can be decomposed by taking the divergence or curl of $\vec{P}(\hat{\mathbf{n}})$ respectively. Density perturbations are scalar metric perturbations, so they have no handedness. They can therefore produce no curl. On the other hand, gravitational waves *do* have a handedness so they can (and we have shown that they do) produce a curl. This therefore provides a way to detect the inflationary stochastic gravity-wave background and thereby test the relations between the inflationary observables. It should also allow one to determine (or at least constrain in the case of a nondetection) the height of the inflaton potential.

More precisely, the Stokes parameters $Q(\hat{\mathbf{n}})$ and $U(\hat{\mathbf{n}})$ (where Q and U are measured with respect to the polar $\hat{\theta}$ and azimuthal $\hat{\phi}$ axes) which specify the linear polarization in direction $\hat{\mathbf{n}}$ are components of a 2×2 symmetric trace-free (STF) tensor,

$$\mathcal{P}_{ab}(\hat{\mathbf{n}}) = \frac{1}{2} \begin{pmatrix} Q(\hat{\mathbf{n}}) & -U(\hat{\mathbf{n}}) \sin \theta \\ -U(\hat{\mathbf{n}}) \sin \theta & -Q(\hat{\mathbf{n}}) \sin^2 \theta \end{pmatrix}, \quad (6)$$

where the subscripts ab are tensor indices. Just as the temperature is expanded in terms of

spherical harmonics, the polarization tensor can be expanded [26],

$$\frac{\mathcal{P}_{ab}(\hat{\mathbf{n}})}{T_0} = \sum_{lm} \left[a_{(lm)}^G Y_{(lm)ab}^G(\hat{\mathbf{n}}) + a_{(lm)}^C Y_{(lm)ab}^C(\hat{\mathbf{n}}) \right], \quad (7)$$

in terms of the tensor spherical harmonics $Y_{(lm)ab}^G$ and $Y_{(lm)ab}^C$, which are a complete basis for the “gradient” (i.e., curl-free) and “curl” components of the tensor field, respectively. The mode amplitudes are given by

$$a_{(lm)}^G = \frac{1}{T_0} \int d\hat{\mathbf{n}} \mathcal{P}_{ab}(\hat{\mathbf{n}}) Y_{(lm)}^{G\,ab*}(\hat{\mathbf{n}}), \quad a_{(lm)}^C = \frac{1}{T_0} \int d\hat{\mathbf{n}} \mathcal{P}_{ab}(\hat{\mathbf{n}}) Y_{(lm)}^{C\,ab*}(\hat{\mathbf{n}}). \quad (8)$$

Here T_0 is the cosmological mean CMB temperature and Q and U are given in brightness temperature units rather than flux units. Scalar perturbations have no handedness. Therefore, they can produce no curl, so $a_{(lm)}^C = 0$ for scalar modes. On the other hand tensor modes *do* have a handedness, so they produce a non-zero curl, $a_{(lm)}^C \neq 0$.

A given inflationary model predicts that the $a_{(lm)}^X$ are gaussian random variables with zero mean, $\langle a_{(lm)}^X \rangle = 0$ (for $X, X' = \{T, G, C\}$) and covariance $\langle (a_{(l'm')}^{X'})^* a_{(lm)}^X \rangle = C_l^{XX'} \delta_{ll'} \delta_{mm'}$. Parity demands that $C_l^{TC} = C_l^{GC} = 0$. Therefore the statistics of the CMB temperature-polarization map are completely specified by the four sets of moments, C_l^{TT} , C_l^{TG} , C_l^{GG} , and C_l^{CC} . Also, as stated above, only tensor modes will produce nonzero C_l^{CC} .

To illustrate, Fig. 5 shows the four temperature-polarization power spectra. The dotted curves correspond to a COBE-normalized inflationary model with cold dark matter and no cosmological constant ($\Lambda = 0$), Hubble constant (in units of $100 \text{ km sec}^{-1} \text{ Mpc}^{-1}$) $h = 0.65$, baryon density $\Omega_b h^2 = 0.024$, scalar spectral index $n_s = 1$, no reionization, and no gravitational waves. The solid curves show the spectra for a COBE-normalized stochastic gravity-wave background with a flat scale-invariant spectrum ($h = 0.65$, $\Omega_b h^2 = 0.024$, and $\Lambda = 0$) in a critical-density Universe. Note that the panel for C_l^{CC} contains no dotted curve since scalar perturbations produce no C polarization component. The dashed curve in the CC panel shows the tensor spectrum for a reionized model with optical depth $\tau = 0.1$ to the surface of last scatter.

As with a temperature map, the sensitivity of a polarization map to gravity waves will be determined by the instrumental noise and fraction of sky covered, and by the angular resolution. Suppose the detector sensitivity is s and the experiment lasts for t_{yr} years with an angular resolution better than 1° . Suppose further that we consider only the CC component of the polarization in our analysis. Then the smallest tensor amplitude \mathcal{T}_{min} to which the experiment will be sensitive at 1σ is [28]

$$\frac{\mathcal{T}_{\text{min}}}{6 C_2^{TT}} \simeq 5 \times 10^{-4} \left(\frac{s}{\mu\text{K} \sqrt{\text{sec}}} \right)^2 t_{\text{yr}}^{-1}. \quad (9)$$

Thus, the curl component of a full-sky polarization map is sensitive to inflaton potentials $V \gtrsim 5 \times 10^{-15} t_{\text{yr}}^{-1} (s/\mu\text{K} \sqrt{\text{sec}})^2$. Improvement on current constraints with only the curl polarization component requires a detector sensitivity $s \lesssim 40 t_{\text{yr}}^{1/2} \mu\text{K} \sqrt{\text{sec}}$. For comparison, the detector sensitivity of MAP will be $s = \mathcal{O}(100 \mu\text{K} \sqrt{\text{sec}})$. However, Planck may conceivably get sensitivities around $s = 25 \mu\text{K} \sqrt{\text{sec}}$.

Eq. (9) is the sensitivity obtained by using only the curl component of the polarization, which provides a model-independent probe of the tensor signal. However, if we are willing to consider specific models for the tensor and scalar spectra, the sensitivity to a tensor signal may be improved somewhat by considering the predictions for the full temperature/polarization auto- and cross-correlation power spectra [28].

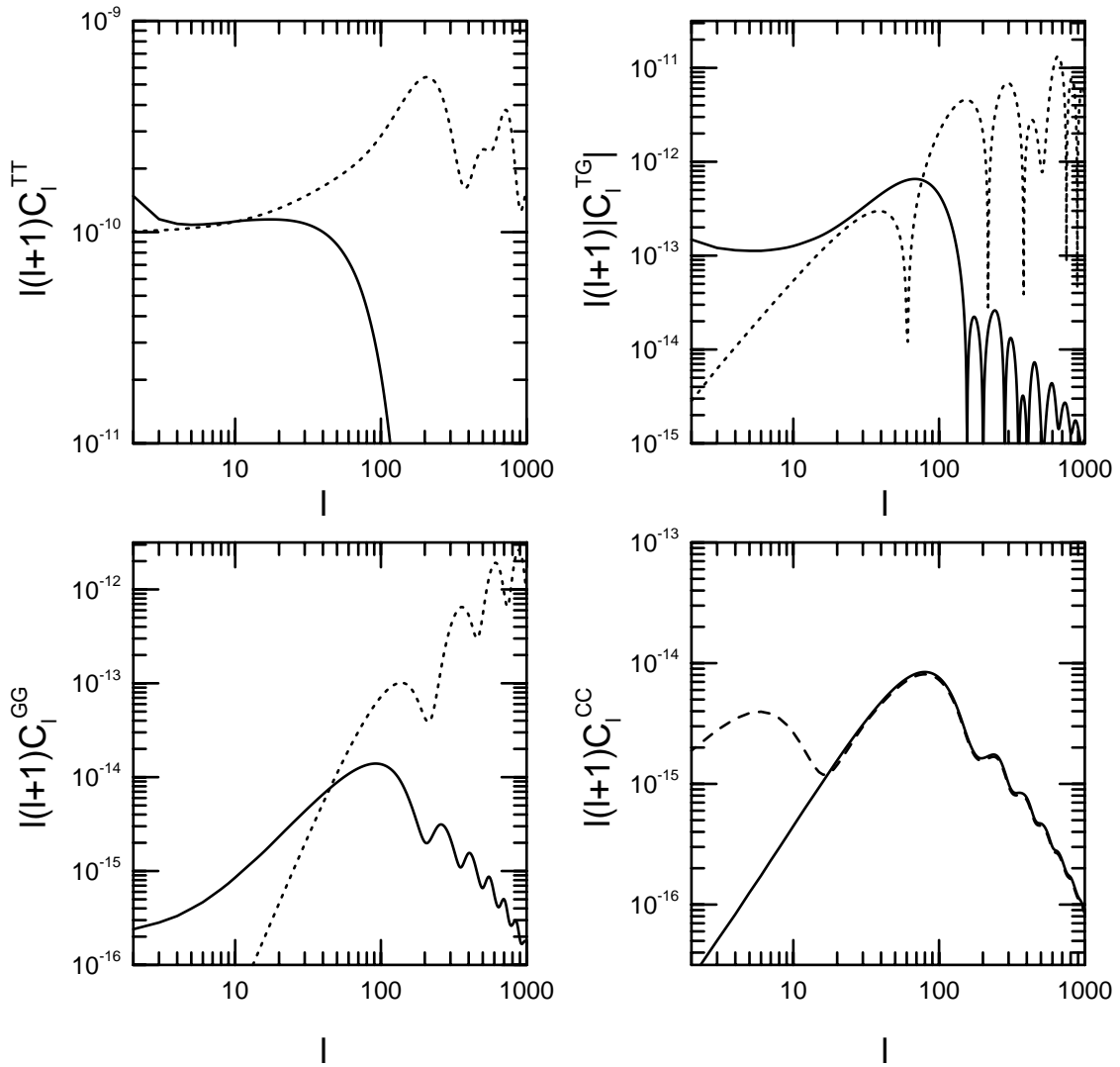


Figure 5: Theoretical predictions for the four nonzero CMB temperature-polarization spectra as a function of multipole moment l . The dashed line in the lower right panel shows a reionized model with optical depth $\tau = 0.1$ to the surface of last scatter.

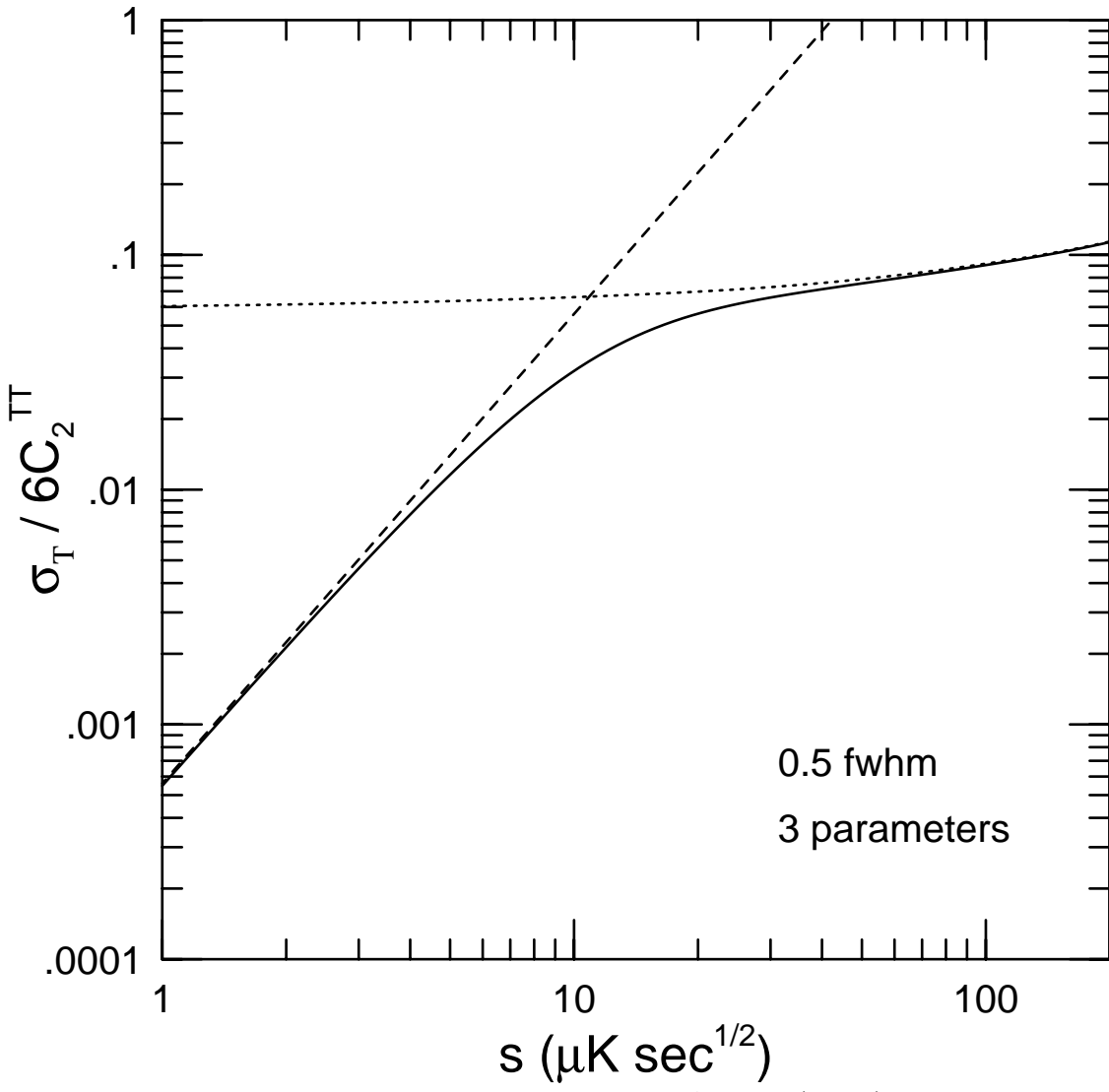


Figure 6: Results for the 1σ sensitivity $\sigma\tau$ to the amplitude \mathcal{T} of a flat ($n_t = 0$) tensor spectrum as a function of detector sensitivity s for an experiment which maps the CMB temperature and polarization on the full sky for one year with an angular resolution of 0.5° . The vertical axis is in units of the temperature quadrupole. See text for more details.

For example, Fig. 6 shows the 1σ sensitivity $\sigma_{\mathcal{T}}$ to the amplitude \mathcal{T} of a flat ($n_t = 0$) tensor spectrum as a function of detector sensitivity s for an experiment which maps the CMB temperature and polarization on the full sky for one year with an angular resolution of 0.5° . The dotted curve shows the results obtained by fitting only the TT moments; the dashed curve shows results obtained by fitting only the CC moments; and the solid curve shows results obtained by fitting all four nonzero sets of moments.

In Fig. 6, we have assumed that the spectra are fit only to \mathcal{S} , \mathcal{T} , and n_s , and the parameters of the cosmological model are those used in Fig. 6. If one fits to more cosmological parameters (e.g., Ω_b , h , Λ , etc.) as well, the the sensitivity from the temperature moments, important for larger s , is degraded. However, the sensitivity due to the CC component, which controls the total sensitivity for smaller s , is essentially unchanged. Again, this is because the CC signal is very model-independent.

For detectors sensitivities $s \gtrsim 20 \mu\text{K} \sqrt{\text{sec}}$, the tensor-mode detectability for the three-parameter fit shown in Fig. 6 comes primarily from the temperature map, although polarization does provides some incremental improvement. However, if the data are fit to more cosmological parameters (not shown), the polarization improves the tensor sensitivity even for $s \gtrsim 20 \mu\text{K} \sqrt{\text{sec}}$. In any case, the sensitivity to tensor modes comes almost entirely from the curl of the polarization for detector sensitivities $s \lesssim 10 \mu\text{K} \sqrt{\text{sec}}$. Since the value of s for Planck will be somewhat higher, it will likely require a more sensitive future experiment to truly capitalize on the model-independent curl signature of tensor modes.

One can also investigate how sensitively the inflationary observables (n_s , n_t , and \mathcal{T}/\mathcal{S}) can be determined by fitting the CMB power spectra measured, e.g., with MAP and Planck, with the CMB, both with and without a polarization map. One can then go one step further and see how precisely the inflaton potential can be reconstructed from these measurements. Ref. [29] addresses these questions very nicely. One finds, that by fitting to all four nonzero sets of power spectra, inclusion of the polarization channels on Planck will provide a dramatic improvement in constraints to inflationary models.

Finally, it should be noted that even a small amount of reionization will significantly increase the polarization signal at low l [30] as shown in the CC panel of Fig. 5 for $\tau = 0.1$. With such a level of reionization [which may be expected in inflation-inspired cold-dark-matter (CDM) models, as discussed in the following Section], the sensitivity to the tensor amplitude is increased by more than a factor of 5 over that in Eq. (9). This level of reionization (if not more) is expected in cold dark matter models [7,31,32], so if anything, Eq. (9) and Fig. 6 provide conservative estimates.

2.4 Other Uses of the Cosmic Microwave Background

The Ostriker-Vishniac Effect and the Epoch of Reionization: Although most of the matter in CDM models does not undergo gravitational collapse until relatively late in the history of the Universe, some small fraction of the mass is expected to collapse at early times. Ionizing radiation released by this early generation of star and/or galaxy formation will partially reionize the Universe, and these ionized electrons will re-scatter at least some cosmic microwave background (CMB) photons after recombination at a redshift of $z \simeq 1100$. Theoretical uncertainties in the process of star formation and the resulting ionization make precise predictions of the ionization history difficult. Constraints to the shape of the CMB blackbody spectrum and detection of CMB anisotropy at degree angular scales suggest that if reionization occurred, the fraction of CMB photons that re-scattered is small. Still, estimates show that even if small, at least some reionization is expected in CDM models [7,31,32]: for example, the most careful recent calculations suggest a fraction $\tau_r \sim 0.1$ of CMB photons were re-scattered [32].

Scattering of CMB photons from ionized clouds will lead to anisotropies at arcminute sep-

arations below the Silk-damping scale (the Ostriker-Vishniac effect) [33,34]. These anisotropies arise at higher order in perturbation theory and are therefore not included in the usual Boltzmann calculations of CMB anisotropy spectra. The level of anisotropy is expected to be small and it has so far eluded detection. However, these anisotropies may be observable with forthcoming CMB interferometry experiments [35] that probe the CMB power spectrum at arcminute scales.

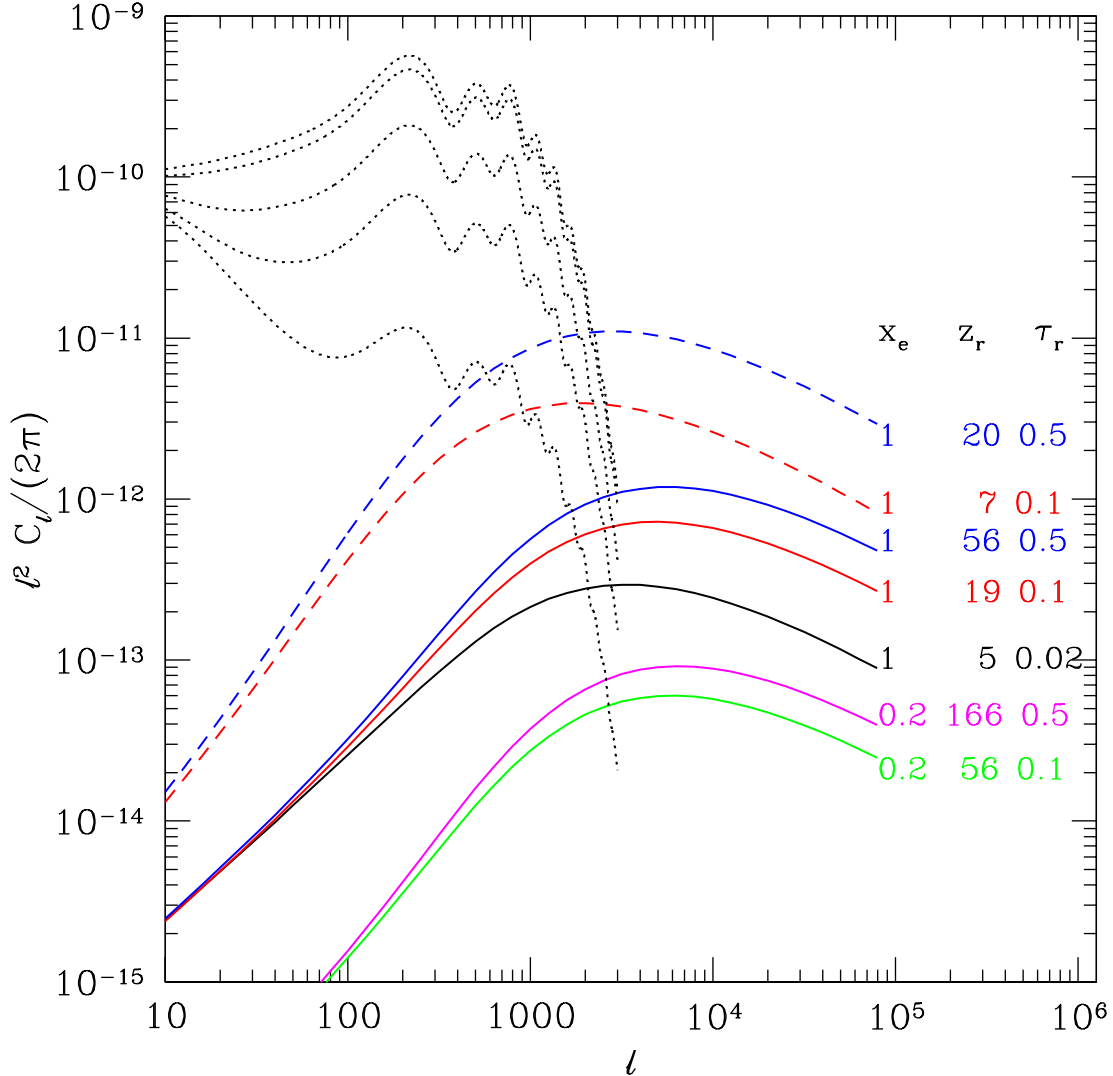


Figure 7: Multipole moments for the Ostriker-Vishniac effect for the COBE-normalized canonical standard-CDM model ($\Omega = 1$, $h = 0.5$, $n = 1$, $\Omega_b h^2 = 0.0125$), for a variety of ionization histories as listed. We also show predictions for several open high-baryon-density models with the same x_e and τ_r , normalized to the cluster abundance, with dashed curves. The dotted curves show the primary anisotropy for this model for $\tau_r = 0.0, 0.1, 0.5, 1$, and 2 , from top to bottom.

Fig. 7 [34] shows the predicted temperature-anisotropy spectrum from the Ostriker-Vishniac effect for a number of ionization histories. The ionization histories are parameterized by an ionization fraction x_e and a redshift z_r at which the Universe becomes reionized. The optical depth τ to the standard-recombination surface of last scatter can be obtained from these two parameters.

Reionization damps the acoustic peaks in the primary-anisotropy spectrum by $e^{-2\tau}$, as shown

in Fig. 7, but this damping is essentially independent of the details of the ionization history. That is, any combination of x_e and z_r that gives the same τ has the same effect on the primary anisotropies. So although MAP and Planck will be able to determine τ from this damping, they will not constrain the epoch of reionization. On the other hand, the secondary anisotropies (the Ostriker-Vishniac anisotropies) produced at smaller angular scales in reionized models *do* depend on the ionization history. For example, although the top and bottom dashed curves in Fig. 7 both have the same optical depth, they have different reionization redshifts ($z_r = 20$ and $z_r = 57$). Therefore, if MAP and Planck determine τ , the amplitude of the Ostriker-Vishniac anisotropy determines the reionization epoch [34].

In a flat Universe, CDM models normalized to cluster abundances produce rms temperature anisotropies of 0.8–2.4 μK on arcminute angular scales for a constant ionization fraction of unity, whereas an ionization fraction of 0.2 yields rms anisotropies of 0.3–0.8 μK [34]. In an open and/or high-baryon-density Universe, the level of anisotropy is somewhat higher. The signal in some of these models may be detectable with planned interferometry experiments [34].

Signatures of New Particle and Gravitational Physics: The CMB may be used as a probe of new particle physics in yet another way: One of the primary goals of experimental particle physics these days is pursuit of a nonzero neutrino mass. Some recent (still controversial) experimental results suggest that one of the neutrinos may have a mass of $\mathcal{O}(5\text{ eV})$ [36], and there have been some (again, still controversial) arguments that such a neutrino mass is just what is required to explain some apparent discrepancies between large-scale-structure observations and the simplest inflation-inspired standard-CDM model [37].

If the neutrino does indeed have a mass of $\mathcal{O}(5\text{ eV})$, then roughly 30% of the mass in the Universe will be in the form of light neutrinos. These neutrinos will affect the growth of gravitational-potential wells near the epoch of last scatter, and they will thus leave an imprint on the CMB angular power spectrum [38]. The effect of a light neutrino on the power spectrum is small, so other cosmological parameters that might affect the shape of the power spectrum at larger l 's must be known well. Still, Ref. [39] argues that by combining measurements of the CMB power spectrum with those of the mass power spectrum measured by, e.g., the Sloan Digital Sky Survey, a neutrino mass of $\mathcal{O}(5\text{ eV})$ can be determined.

The CMB may also conceivably be used to test alternative gravity theories [40,41] such as Jordan-Brans-Dicke or more general scalar-tensor theories. The idea here is that in such a theory, the expansion rate at the epoch of last scatter will be different, and this will provide a unique signature in the CMB power spectrum.

Cross-Correlation with the x-ray background: In an Einstein-de Sitter Universe, large-angle CMB anisotropies are produced by gravitational-potential differences induced by density perturbations at the surface of last scatter at a redshift $z \simeq 1100$ via the Sachs-Wolfe (SW) effect. In a flat cosmological-constant Universe [42], or in an open Universe [7], additional anisotropies are produced by density perturbations at lower redshifts along the line of sight via the integrated Sachs-Wolfe (ISW) effect. Crittenden and Turok [43] thus argued that in a flat cosmological-constant Universe, there should be some cross-correlation between the CMB and a tracer of the mass distribution at low redshifts; a similar cross-correlation should also arise in an open Universe [44].

The x-ray background (XRB) currently offers perhaps the best tracer of the mass distribution out to redshifts of a few. Boughn, Crittenden, and Turok [45] determined an upper limit to the amplitude of the cross-correlation between the Cosmic Background Explorer (COBE) CMB map and the first High-Energy Astrophysical Observatory (HEAO I) map of the 2–20 keV XRB, and used it to constrain $\Omega_0 \gtrsim 0.3$ in a flat cosmological-constant Universe. More recently, the analogous calculation has been carried out for an open Universe [46]. It is found that in an open Universe with a nearly scale-invariant spectrum of primordial adiabatic perturbations, $\Omega_0 \gtrsim 0.7$. This result makes open-CDM models with $\Omega_0 \simeq 0.3 - 0.4$ unlikely.

3 Dark Matter and New Particles

3.1 The Local Dark-Matter Density

The extent of the luminous disk of our Galaxy, the Milky Way, is roughly 10 kpc, and we live about 8.5 kpc from the center. Due to our location *in* it, the rotation curve of the Milky Way cannot be determined with the same precision as that of an external spiral galaxy, such as that shown in Fig. 1. However, it is qualitatively the same. The circular speed rises linearly from zero at the center and asymptotes to roughly 220 km sec^{-1} somewhere near our own Galactocentric radius and remains roughly flat all the way out to ~ 25 kpc. Although direct measurements of the rotation curve are increasingly difficult at larger radii, the orbital motions of satellites of the Milky Way suggest that the rotation curve remains constant all the way out to radii of 50 kpc and perhaps even farther. According to Newton's laws, the rotation speed should fall as $v_c \propto r^{-1/2}$ at radii greater than the extent of the luminous disk. However, it is observed to remain flat to much larger distances. It therefore follows that the luminous disk and bulge must be immersed in an extended dark halo (or that Newton's laws are violated).

Our knowledge of the halo comes almost solely from this rotation curve. Therefore, we do not know empirically if the halo is round, elliptical, or perhaps flattened like the disk. However, there are good reasons to believe that the halo should be much more diffuse than the disk. The disk is believed to be flat because luminous matter can radiate photons and therefore gravitationally collapse to a pancake-like structure. On the other hand, dark matter (by definition) cannot radiate photons. There are also now empirical arguments which involve, e.g., the shape of the distribution of gas in the Milky Way, which suggest that the dark halo should be much more diffuse than the disk [47].

Assuming that the halo is therefore nearly round, it must have a density distribution like

$$\rho(r) = \rho_0 \frac{r_0^2 + a^2}{r^2 + a^2}, \quad (10)$$

where r is the radius, $r_0 \simeq 8.5$ kpc is our distance from the center, a is a to-be-determined core radius of the halo, and ρ_0 is the local halo density. Such a halo would give rise to a rotation curve,

$$v_h^2(r) = 4\pi G \rho_0 (r_0^2 + a^2) \left[1 - \left(\frac{a}{r} \right) \tan^{-1} \left(\frac{a}{r} \right) \right], \quad (11)$$

where G is Newton's constant. If we know the rotation speed contributed by the halo at two points, we can determine ρ_0 and a . At large radii, the rotation curve of the Milky Way is supported entirely by this dark halo, so $v_h(r \gg 10 \text{ kpc}) \simeq 220 \text{ km sec}^{-1}$. However, the rotation curve locally is due in part to the disk, $v_c^2(r_0) = v_d^2(r_0) + v_h^2(r_0)$. The disk contribution to the local rotation speed is somewhat uncertain but probably falls in the range $v_d(r_0) \simeq 118\text{--}155 \text{ km sec}^{-1}$, which means that the halo contribution to the local rotation speed is $v_h(r_0) \simeq 150\text{--}185 \text{ km sec}^{-1}$. Given the local and asymptotic rotation speeds, we infer that the local halo density is $\rho_0 \simeq 0.3\text{--}0.5 \text{ GeV cm}^{-3}$. The particles which make up the dark halo move locally in the same gravitational potential well as the Sun. Therefore, the virial theorem tells us that they must move with velocities $v \sim v_c \sim 220 \text{ km sec}^{-1}$. Additional theoretical arguments suggest that the velocity distribution of these particles is locally nearly isotropic and nearly a Maxwell-Boltzmann distribution, (although the assumption of a Maxwell-Boltzmann distribution will not affect the detection rates discussed below [48]). To sum, application of Newton's laws to our Galaxy tells us that the luminous disk and bulge must be immersed in a dark halo with a local density $\rho_0 \simeq 0.4 \text{ GeV cm}^{-3}$ and that dark-matter particles (whatever they are) move with velocities comparable to the local circular speed. More careful investigations along these lines show that similar conclusions are reached even if we allow for the possibility of a slightly flattened halo or a radial distribution which differs from that in Eq. (10) [48].

3.2 Axions

Although supersymmetric particles seem to get more attention in the literature lately, we should not forget that the axion also provides a well-motivated and promising alternative dark-matter candidate [12]. The QCD Lagrangian may be written

$$\mathcal{L}_{QCD} = \mathcal{L}_{\text{pert}} + \theta \frac{g^2}{32\pi^2} G\tilde{G}, \quad (12)$$

where the first term is the perturbative Lagrangian responsible for the numerous phenomenological successes of QCD. However, the second term (where G is the gluon field-strength tensor and \tilde{G} is its dual), which is a consequence of nonperturbative effects, violates CP . However, we know experimentally that CP is not violated in the strong interactions, or if it is, the level of strong- CP violation is tiny. From constraints to the neutron electric-dipole moment, $d_n \lesssim 10^{-25}$ e cm, it can be inferred that $\theta \lesssim 10^{-10}$. But why is θ so small? This is the strong- CP problem.

The axion arises in the Peccei-Quinn solution to the strong- CP problem [49], which close to twenty years after it was proposed still seems to be the most promising solution. The idea is to introduce a global $U(1)_{PQ}$ symmetry broken at a scale f_{PQ} , and θ becomes a dynamical field which is the Nambu-Goldstone mode of this symmetry. At temperatures below the QCD phase transition, nonperturbative quantum effects break explicitly the symmetry and drive $\theta \rightarrow 0$. The axion is the pseudo-Nambu-Goldstone boson of this near-global symmetry. Its mass is $m_a \simeq \text{eV} (10^7 \text{ GeV}/f_a)$, and its coupling to ordinary matter is $\propto f_a^{-1}$.

A priori, the Peccei-Quinn solution works equally well for any value of f_a (although one would generically expect it to be less than or of order the Planck scale). However, a variety of astrophysical observations and a few laboratory experiments constrain the axion mass to be $m_a \sim 10^{-4}$ eV, to within a few orders of magnitude. Smaller masses would lead to an unacceptably large cosmological abundance. Larger masses are ruled out by a combination of constraints from supernova 1987A, globular clusters, laboratory experiments, and a search for two-photon decays of relic axions [50].

One conceivable theoretical difficulty with this axion mass comes from generic quantum-gravity arguments [51]. For $m_a \sim 10^{-4}$ eV, the magnitude of the explicit symmetry breaking is incredibly tiny compared with the PQ scale, so the global symmetry, although broken, must be very close to exact. There are physical arguments involving, for example, the nonconservation of global charge in evaporation of a black hole produced by collapse of an initial state with nonzero global charge, which suggest that global symmetries should be violated to some extent in quantum gravity. When one writes down a reasonable *ansatz* for a term in a low-energy effective Lagrangian which might arise from global-symmetry violation at the Planck scale, the coupling of such a term is found to be extraordinarily small (e.g., $\lesssim 10^{-55}$). Of course, we have at this point no predictive theory of quantum gravity, and several mechanisms for forbidding these global-symmetry violating terms have been proposed [52]. Therefore, these arguments by no means “rule out” the axion solution. In fact, discovery of an axion would provide much needed clues to the nature of Planck-scale physics.

Curiously enough, if the axion mass is in the relatively small viable range, the relic density is $\Omega_a \sim 1$ and may therefore account for the halo dark matter. Such axions would be produced with zero momentum by a misalignment mechanism in the early Universe and therefore act as cold dark matter. During the process of galaxy formation, these axions would fall into the Galactic potential well and would therefore be present in our halo with a velocity dispersion near 270 km sec^{-1} .

Although the interaction of axions with ordinary matter is extraordinarily weak, Sikivie proposed a very clever method of detection of Galactic axions [53]. Just as the axion couples to gluons through the anomaly (i.e., the $G\tilde{G}$ term), there is a very weak coupling of an axion to photons through the anomaly. The axion can therefore decay to two photons, but the lifetime

is $\tau_{a \rightarrow \gamma\gamma} \sim 10^{50} \text{ s } (m_a/10^{-5} \text{ eV})^{-5}$ which is huge compared to the lifetime of the Universe and therefore unobservable. However, the $a\gamma\gamma$ term in the Lagrangian is $\mathcal{L}_{a\gamma\gamma} \propto a \vec{E} \cdot \vec{B}$ where \vec{E} and \vec{B} are the electric and magnetic field strengths. Therefore, if one immerses a resonant cavity in a strong magnetic field, Galactic axions which pass through the detector may be converted to fundamental excitations of the cavity, and these may be observable [53]. Such an experiment is currently underway [54]. They have already begun to probe part of the cosmologically interesting parameter space (no, they haven't found anything yet) and expect to cover most of the interesting region parameter space in the next three years. A related experiment, which looks for excitations of Rydberg atoms, may also find dark-matter axions [55]. Although the sensitivity of this technique should be excellent, it can only cover a limited axion-mass range.

It should be kept in mind that there are no accelerator tests for axions in the acceptable mass range. Therefore, these dark-matter axion experiment are actually our *only* way to test the Peccei-Quinn solution.

3.3 Weakly-Interacting Massive Particles

Suppose that in addition to the known particles of the standard model, there exists a new, yet undiscovered, stable (or long-lived) weakly-interacting massive particle (WIMP), χ . At temperatures greater than the mass of the particle, $T \gg m_\chi$, the equilibrium number density of such particles is $n_\chi \propto T^3$, but for lower temperatures, $T \ll m_\chi$, the equilibrium abundance is exponentially suppressed, $n_\chi \propto e^{-m_\chi/T}$. If the expansion of the Universe were so slow that thermal equilibrium was always maintained, the number of WIMPs today would be infinitesimal. However, the Universe is not static, so equilibrium thermodynamics is not the entire story.

At high temperatures ($T \gg m_\chi$), χ 's are abundant and rapidly converting to lighter particles and *vice versa* ($\chi\bar{\chi} \leftrightarrow l\bar{l}$, where $l\bar{l}$ are quark-antiquark and lepton-antilepton pairs, and if m_χ is greater than the mass of the gauge and/or Higgs bosons, $l\bar{l}$ could be gauge- and/or Higgs-boson pairs as well). Shortly after T drops below m_χ the number density of χ 's drops exponentially, and the rate for annihilation of χ 's, $\Gamma = \langle\sigma v\rangle n_\chi$ —where $\langle\sigma v\rangle$ is the thermally averaged total cross section for annihilation of $\chi\bar{\chi}$ into lighter particles times relative velocity v —drops below the expansion rate, $\Gamma \lesssim H$. At this point, the χ 's cease to annihilate, they fall out of equilibrium, and a relic cosmological abundance remains.

Fig. 8 shows numerical solutions to the Boltzmann equation which determines the WIMP abundance. The equilibrium (solid line) and actual (dashed lines) abundances per comoving volume are plotted as a function of $x \equiv m_\chi/T$ (which increases with increasing time). As the annihilation cross section is increased the WIMPs stay in equilibrium longer, and we are left with a smaller relic abundance.

An approximate solution to the Boltzmann equation yields the following estimate for the current cosmological abundance of the WIMP:

$$\Omega_\chi h^2 = \frac{m_\chi n_\chi}{\rho_c} \simeq \left(\frac{3 \times 10^{-27} \text{ cm}^3 \text{ sec}^{-1}}{\sigma_{A} v} \right), \quad (13)$$

where h is the Hubble constant in units of $100 \text{ km sec}^{-1} \text{ Mpc}^{-1}$. The result is to a first approximation independent of the WIMP mass and is fixed primarily by its annihilation cross section.

The WIMP velocities at freeze out are typically some appreciable fraction of the speed of light. Therefore, from Eq. (13), the WIMP will have a cosmological abundance of order unity today if the annihilation cross section is roughly 10^{-9} GeV^{-2} . Curiously, this is the order of magnitude one would expect from a typical electroweak cross section,

$$\sigma_{\text{weak}} \simeq \frac{\alpha^2}{m_{\text{weak}}^2}, \quad (14)$$

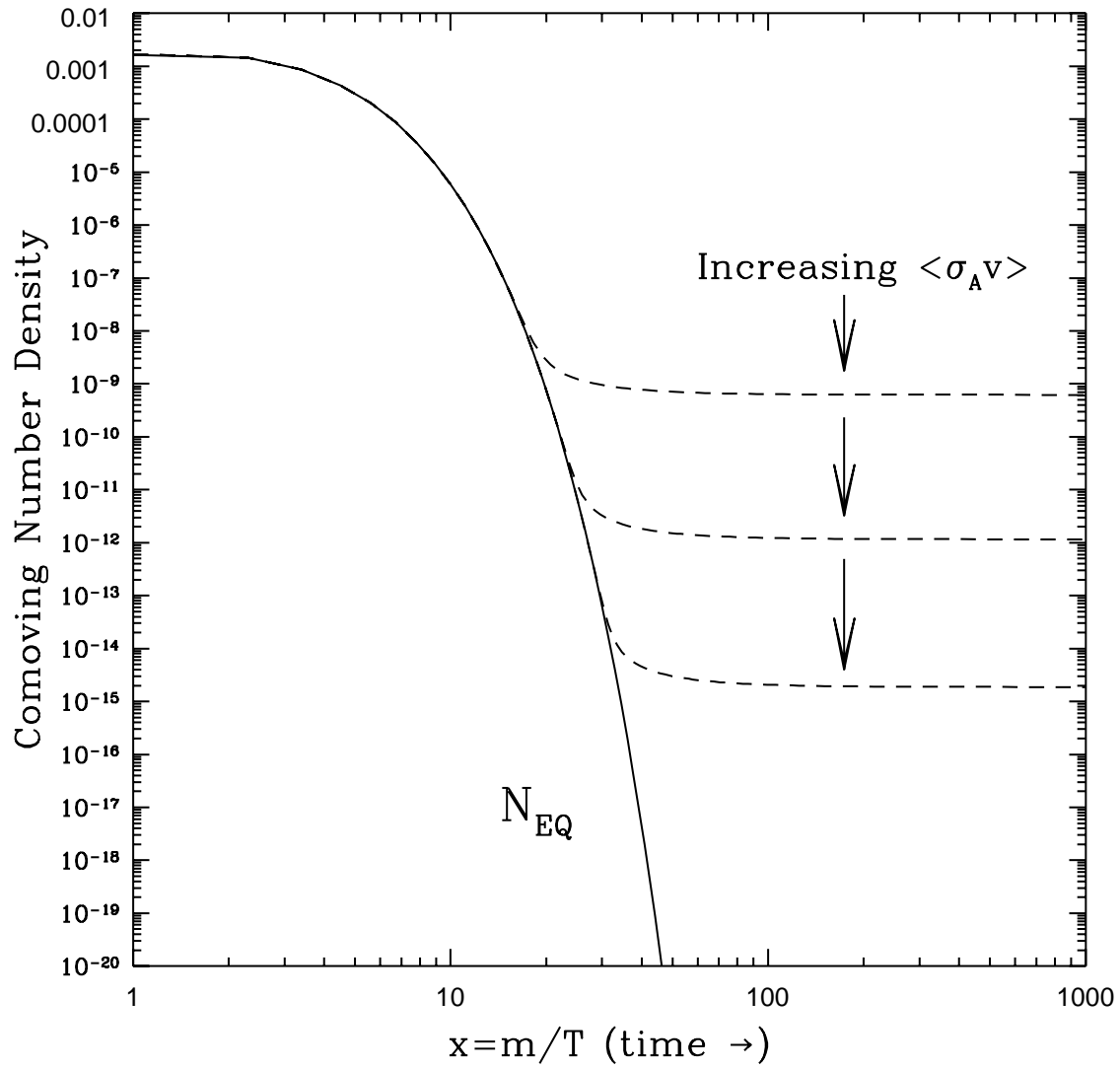


Figure 8: Comoving number density of a WIMP in the early Universe. The dashed curves are the actual abundance, and the solid curve is the equilibrium abundance.

where $\alpha \simeq \mathcal{O}(0.01)$ and $m_{\text{weak}} \simeq \mathcal{O}(100 \text{ GeV})$. The value of the cross section in Eq. (13) needed to provide $\Omega_\chi \sim 1$ comes essentially from the age of the Universe. However, there is no *a priori* reason why this cross section should be of the same order of magnitude as the cross section one would expect for new particles with masses and interactions characteristic of the electroweak scale. In other words, why should the age of the Universe have anything to do with electroweak physics? This “coincidence” suggests that if a new, yet undiscovered, massive particle with electroweak interactions exists, then it should have a relic density of order unity and therefore provides a natural dark-matter candidate. This argument has been the driving force behind a vast effort to detect WIMPs in the halo.

The first WIMPs considered were massive Dirac or Majorana neutrinos with masses in the range of a few GeV to a few TeV. (Due to the Yukawa coupling which gives a neutrino its mass, the neutrino interactions become strong above a few TeV, and it no longer remains a suitable WIMP candidate [56].) LEP ruled out neutrino masses below half the Z^0 mass. Furthermore, heavier Dirac neutrinos have been ruled out as the primary component of the Galactic halo by direct-detection experiments (described below) [57], and heavier Majorana neutrinos have been ruled out by indirect-detection experiments [58] (also described below) over much of their mass range. Therefore, Dirac neutrinos cannot comprise the halo dark matter [59]; Majorana neutrinos can, but only over a small range of fairly large masses. This was a major triumph for experimental particle astrophysicists: the first falsification of a dark-matter candidate. However, theorists were not too disappointed: The stability of a fourth-generation neutrino had to be postulated *ad hoc*—it was not guaranteed by some new symmetry. So although heavy neutrinos were plausible, they certainly were not very well-motivated from the perspective of particle theory.

Supersymmetric Dark Matter: A much more promising WIMP candidate comes from supersymmetry (SUSY) [13,60]. SUSY was hypothesized in particle physics to cure the naturalness problem with fundamental Higgs bosons at the electroweak scale. Coupling-constant unification at the GUT scale seems to be improved with SUSY, and it seems to be an essential ingredient in theories which unify gravity with the other three fundamental forces.

As another consequence, the existence of a new symmetry, R -parity, in SUSY theories guarantees that the lightest supersymmetric particle (LSP) is stable. In the minimal supersymmetric extension of the standard model (MSSM), the LSP is usually the neutralino, a linear combination of the supersymmetric partners of the photon, Z^0 , and Higgs bosons. (Another possibility is the sneutrino, but these particles interact like neutrinos and have been ruled out over most of the available mass range [61].) Given a SUSY model, the cross section for neutralino annihilation to lighter particles is straightforward, so one can obtain the cosmological mass density. The mass scale of supersymmetry must be of order the weak scale to cure the naturalness problem, and the neutralino will have only electroweak interactions. Therefore, it is to be expected that the cosmological neutralino abundance is of order unity. In fact, with detailed calculations, one finds that the neutralino abundance in a very broad class of supersymmetric extensions of the standard model is near unity and can therefore account for the dark matter in our halo [62].

This is illustrated in Fig. 9 where the cosmological abundance Ω_χ (times h^2) is plotted versus the neutralino mass Ω_χ . Each point represent one supersymmetric model, or equivalently, one choice of the MSSM parameters. Models with $\Omega_\chi h^2 \gtrsim 1$ are inconsistent with a conservative lower bound (10 Gyr) to the age of the Universe, and those with $\Omega_\chi h^2 \lesssim 0.025$ are cosmologically consistent, but probably too scarce to account for the dark matter in galactic halos. Still, numerous models have an abundance between these two limits, and these models make excellent dark-matter candidates.

Direct Detection: If neutralinos reside in the halo, there are several avenues toward detection [13]. One of the most promising techniques currently being pursued involves searches for the $\mathcal{O}(10 \text{ keV})$ recoils produced by elastic scattering of neutralinos from nuclei in low-background

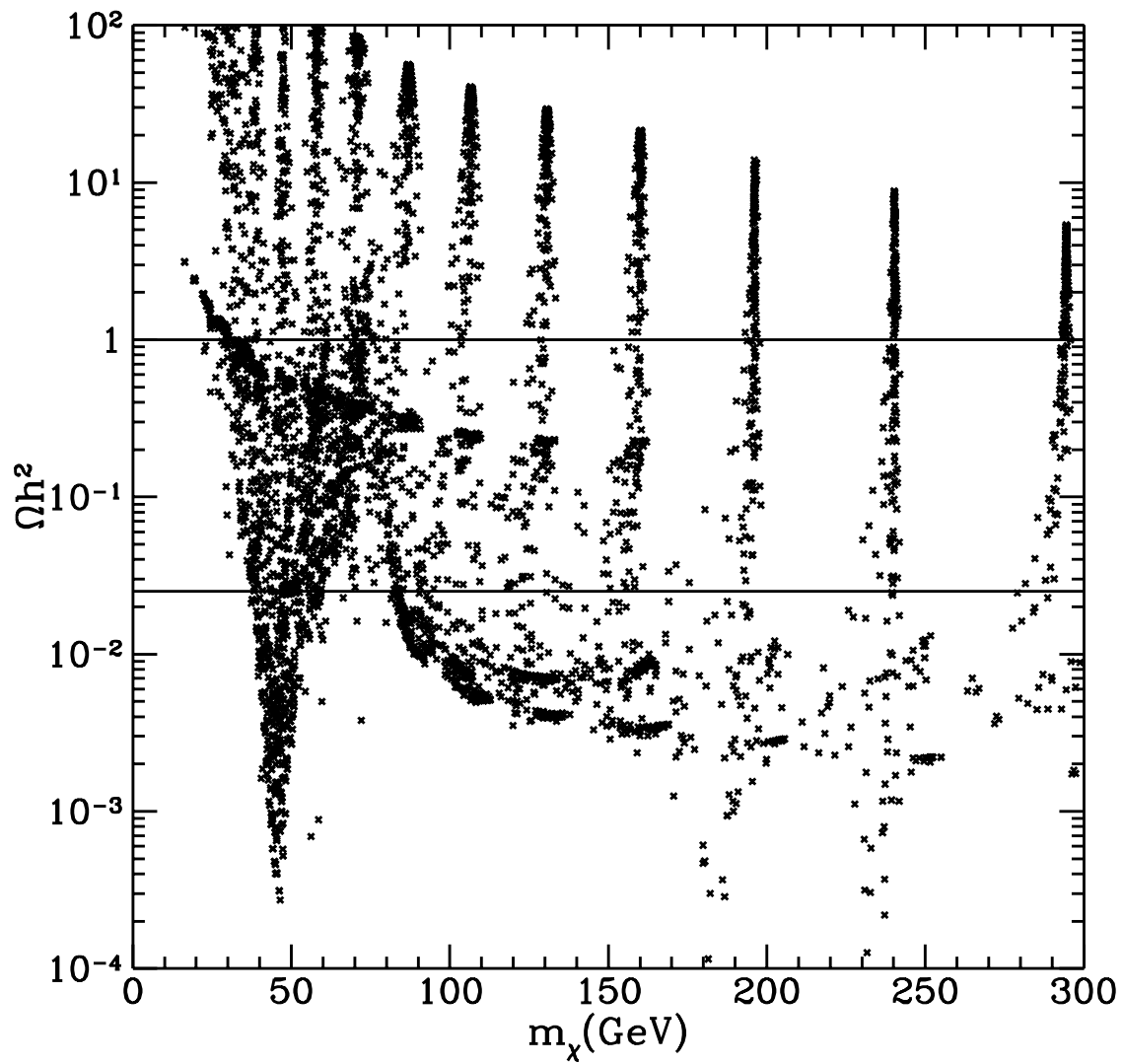


Figure 9: Cosmological abundance of a WIMP versus the WIMP mass. Each point represents the result for a given choice of the MSSM parameters. From Ref. [13].

detectors [63,64]. The idea here is simple. A particle with mass $m_\chi \sim 100$ GeV and electroweak-scale interactions will have a cross section for elastic scattering from a nucleus which is $\sigma \sim 10^{-38}$ cm². If the local halo density is $\rho_0 \simeq 0.4$ GeV cm⁻³, and the particles move with velocities $v \sim 300$ km sec⁻¹, then the rate for elastic scattering of these particles from, e.g., germanium which has a mass $m_N \sim 70$ GeV, will be $R \sim \rho_0 \sigma v / m_\chi / m_N \sim 1$ event kg⁻¹ yr⁻¹. If a 100-GeV WIMP moving at $v/c \sim 10^{-3}$ elastically scatters with a nucleus of similar mass, it will impart a recoil energy up to 100 keV to the nucleus. Therefore, if we have 1 kg of germanium, we expect to see roughly one nucleus per year spontaneously recoil with an energy nearly 100 keV.

Of course, this is only a *very* rough calculation. To do the calculation more precisely, one needs to use a proper neutralino-quark interaction, treat the QCD and nuclear physics which takes you from a neutralino-quark interaction to a neutralino-nucleus interaction, and integrate over the WIMP velocity distribution. Even if all of these physical effects are included properly, there is still a significant degree of uncertainty in the predicted event rates. Although supersymmetry provides perhaps the most promising dark-matter candidate (and solves numerous problems in particle physics), it really provides little detailed predictive power. In SUSY models, the standard-model particle spectrum is more than doubled, and we really have no idea what the masses of all these superpartners should be. There are also couplings, mixing angles, etc. Therefore, what theorists generally do is survey a large set of models with masses and couplings within a plausible range, and present results for relic abundances and direct- and indirect-detection rates, usually as scatter plots versus neutralino mass.

After taking into account all the relevant physical effects and surveying the plausible region of SUSY parameter space, one generally finds that the predicted event rates seem to fall for the most part between 10^{-4} to 10 events kg⁻¹ day⁻¹ [13], as shown in Fig. 10 although again, there may be models with higher or lower rates. Current experimental sensitivities in germanium detectors are around 10 events kg⁻¹ day⁻¹ [57]. To illustrate future prospects, consider the CDMS experiment [65] which expects to soon have a kg germanium detector with a background rate of 1 event day⁻¹. After a one-year exposure, their sensitivity would therefore be $\mathcal{O}(0.1 \text{ event kg}^{-1} \text{ day}^{-1})$; this could be improved with better background rejection. Future detectors will achieve better sensitivities, and it should be kept in mind that numerous other target nuclei are being considered by other groups. However, it also seems clear that it will be quite a while until a good fraction of the available SUSY parameter space is probed.

Indirect Detection: Another strategy is observation of energetic neutrinos produced by annihilation of neutralinos in the Sun and/or Earth in converted proton-decay and astrophysical-neutrino detectors (such as MACRO, Kamiokande, IMB, AMANDA, and NESTOR) [66]. If, upon passing through the Sun, a WIMP scatters elastically from a nucleus therein to a velocity less than the escape velocity, it will be gravitationally bound in the Sun. This leads to a significant enhancement in the density of WIMPs in the center of the Sun—or by a similar mechanism, the Earth. These WIMPs will annihilate to, e.g., c , b , and/or t quarks, and/or gauge and Higgs bosons. Among the decay products of these particles will be energetic muon neutrinos which can escape from the center of the Sun and/or Earth and be detected in neutrino telescopes such as IMB, Kamiokande, MACRO, AMANDA, or NESTOR. The energies of these muons will be typically 1/3 to 1/2 the neutralino mass (e.g., 10s to 100s of GeV) so they will be much more energetic—and therefore cannot be confused with—ordinary solar neutrinos. The signature of such a neutrino would be the Cerenkov radiation emitted by an upward muon produced by a charged-current interaction between the neutrino and a nucleus in the rock below the detector.

The annihilation rate of these WIMPs is equal to the rate for capture of these particles in the Sun. This can be estimated in order of magnitude by determining the rate at which halo WIMPs elastically scatter from nuclei in the Sun. The flux of neutrinos at the Earth depends also on the Earth-Sun distance, WIMP annihilation branching ratios, and the decay branching ratios of the annihilation products. The flux of upward muons depends on the flux of neutrinos

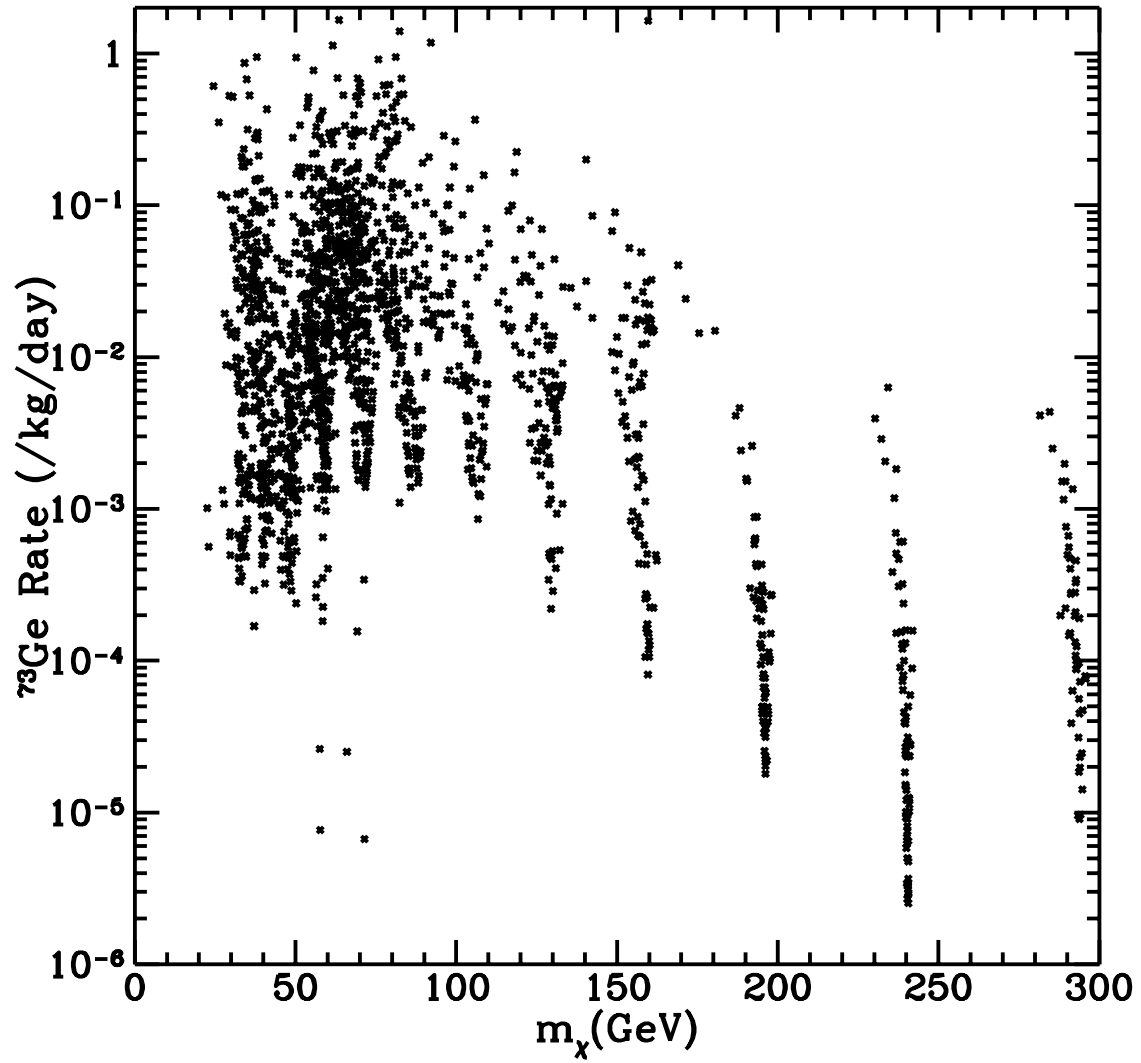


Figure 10: Rates for direct detection of neutralinos of mass m_χ in a ^{73}Ge detector. From Ref. [13].

and the cross section for production of muons, which depends on the square of the neutrino energy.

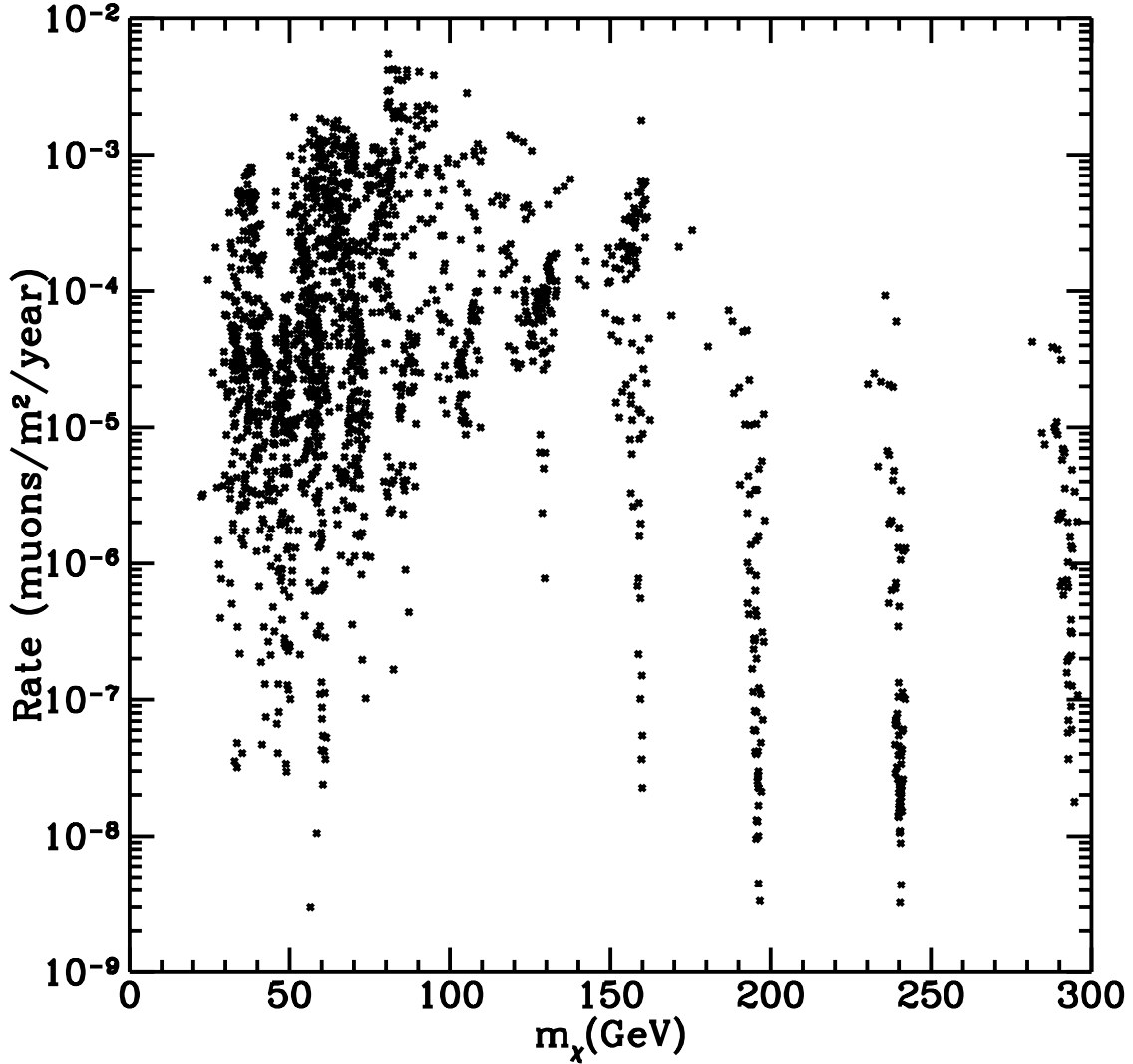


Figure 11: Rates for indirect detection of neutralinos of mass m_χ via observation of energetic neutrinos from annihilation in the Sun and Earth. From Ref. [13].

As in the case of direct detection, the precise prediction involves numerous factors from particle and nuclear physics and astrophysics, and on the SUSY parameters. When all these factors are taken into account, predictions for the fluxes of such muons in SUSY models seem to fall for the most part between 10^{-6} and 1 event $\text{m}^{-2} \text{yr}^{-1}$ [13], as shown in Fig. 11, although the numbers may be a bit higher or lower in some models. Presently, IMB and Kamiokande constrain the flux of energetic neutrinos from the Sun to be less than about $0.02 \text{ m}^{-2} \text{yr}^{-1}$ [58,67], and the Baksan limit is perhaps a factor-of-two better [68]. MACRO expects to be able to improve on this sensitivity by perhaps an order of magnitude. Future detectors may be able to improve even further. For example, AMANDA expects to have an area of roughly 10^4 m^2 , and a 10^6-m^2 detector is being discussed. However, it should be kept in mind that without muon energy resolution, the sensitivity of these detectors will not approach the inverse exposure; it will be limited by the atmospheric-neutrino background. If a detector has good angular

resolution, the signal-to-noise ratio can be improved, and even moreso with energy resolution, so sensitivities approaching the inverse exposure could be achieved [69]. Furthermore, ideas for neutrino detectors with energy resolution are being discussed [70], although at this point these appear likely to be in the somewhat-distant future.

Direct/Indirect Comparison: With two promising avenues toward detection, it is natural to inquire which is most promising. Due to the abundance of undetermined SUSY parameters and the complicated dependence of event rates on these parameters, the answer to this question is not entirely straightforward. Generally, most theorists have just plugged SUSY parameters into the machinery which produces detection rates and plotted results for direct and indirect detection. However, another approach is to compare, in a somewhat model-independent although approximate fashion, the rates for direct and indirect detection [13,71,72]. The underlying observation is that the rates for the two types of detection are both controlled primarily by the WIMP-nucleon coupling. One must then note that WIMPs generally undergo one of two types of interaction with the nucleon: an axial-vector interaction in which the WIMP couples to the nuclear spin (which, for nuclei with nonzero angular momentum is roughly 1/2 and *not* the total angular momentum), and a scalar interaction in which the WIMP couples to the total mass of the nucleus. The direct-detection rate depends on the WIMP-nucleon interaction strength and on the WIMP mass. On the other hand, indirect-detection rates will have an additional dependence on the energy spectrum of neutrinos from WIMP annihilation. By surveying the various possible neutrino energy spectra, one finds that for a given neutralino mass and annihilation rate in the Sun, the largest upward-muon flux is roughly three times as large as the smallest [72]. So even if we assume the neutralino-nucleus interaction is purely scalar or purely axial-vector, there will still be a residual model-dependence of a factor of three when comparing direct- and indirect-detection rates.

For example, for scalar-coupled WIMPs, the event rate in a kg germanium detector will be equivalent to the event rate in a $(2 - 6) \times 10^6$ m² neutrino detector for 10-GeV WIMPs and $(3-5) \times 10^4$ m² for TeV WIMPs [72]. Therefore, the relative sensitivity of indirect detection when compared with the direct-detection sensitivity increases with mass. The bottom line of such an analysis seems to be that direct-detection experiments will be more sensitive to neutralinos with scalar interactions with nuclei, although very-large neutrino telescopes may achieve comparable sensitivities at larger WIMP masses. This should come as no surprise given the fact that direct-detection experiments rule out Dirac neutrinos [57], which have scalar-like interactions, far more effectively than do indirect-detection experiments [72].

Generically, the sensitivity of indirect searches (relative to direct searches) should be better for WIMPs with axial-vector interactions, since the Sun is composed primarily of nuclei with spin (i.e., protons). However, a comparison of direct- and indirect-detection rates is a bit more difficult for axially-coupled WIMPs, since the nuclear-physics uncertainties in the neutralino-nuclear cross section are much greater, and the spin distribution of each target nucleus must be modeled. Still, in a careful analysis, Rich and Tao found that in 1994, the existing sensitivity of energetic-neutrino searches to axially-coupled WIMPs greatly exceeded the sensitivities of direct-detection experiments [71].

To see how the situation may change with future detectors, let us consider a specific axially-coupled dark-matter candidate, the light Higgsino recently put forward by Kane and Wells [73]. Even if this candidate is inconsistent, it will serve as a toy model for a WIMP with primarily spin-dependent interactions. In order to explain the anomalous CDF $ee\gamma\gamma + \cancel{E}_T$ [74], the $Z \rightarrow b\bar{b}$ anomaly, and the dark matter, this Higgsino must have a mass between 30-40 GeV. Furthermore, the coupling of this Higgsino to quarks and leptons is due primarily to Z^0 exchange with a coupling proportional to $\cos 2\beta$, where $\tan \beta$ is the usual ratio of Higgs vacuum expectation values in supersymmetric models. Therefore, the usually messy cross sections one deals with in a general MSSM simplify for this candidate, and the cross sections needed for the

cosmology of this Higgsino depend only on the two parameters m_χ and $\cos 2\beta$. Furthermore, since the neutralino-quark interaction is due only to Z^0 exchange, this Higgsino will have only axial-vector interactions with nuclei.

The Earth is composed primarily of spinless nuclei, so WIMPs with axial-vector interactions will not be captured in the Earth, and we expect no neutrinos from WIMP annihilation therein. However, most of the mass in the Sun is composed of nuclei with spin (i.e., protons). The flux of upward muons induced by neutrinos from annihilation of these light Higgsinos would be $\Gamma_{\text{det}} \simeq 2.7 \times 10^{-2} \text{ m}^{-2} \text{ yr}^{-1} \cos^2 2\beta$ [75]. On the other hand, the rate for scattering from ^{73}Ge is $R \simeq 300 \cos^2 2\beta \text{ kg}^{-1} \text{ yr}^{-1}$ [73,75]. For illustration, in addition to their kg of natural germanium, the CDMS experiment also plans to run with 0.5 kg of (almost) purified ^{73}Ge . With a background event rate of roughly one event $\text{kg}^{-1} \text{ day}^{-1}$, after one year, the 3σ sensitivity of the experiment will be roughly $80 \text{ kg}^{-1} \text{ yr}^{-1}$. Comparing the predictions for direct and indirect detection of this axially-coupled WIMP, we see that the enriched- ^{73}Ge sensitivity should improve on the *current* limit to the upward-muon flux ($0.02 \text{ m}^{-2} \text{ yr}^{-1}$) roughly by a factor of 4. When we compare this with the forecasted factor-of-ten improvement expected in MACRO, it appears that the sensitivity of indirect-detection experiments looks more promising. Before drawing any conclusions, however, it should be noted that the sensitivity in detectors with other nuclei with spin may be significantly better. On the other hand, the sensitivity of neutrino searches increases relative to direct-detection experiments for larger WIMP masses. It therefore seems at this point that the two schemes will be competitive for detection of light axially-coupled WIMPs, but the neutrino telescopes may have an advantage in probing larger masses.

A common question is whether theoretical considerations favor a WIMP which has predominantly scalar interactions or whether they favor axial-vector couplings. Unfortunately, there is no simple answer. When detection of supersymmetric dark matter was initially considered, it seemed that the neutralino in most models would have predominantly axial-vector interactions. It was then noted that in some fraction of models where the neutralino was a mixture of Higgsino and gaugino, there could be some significant scalar coupling as well [76]. As it became evident that the top quark had to be quite heavy, it was realized that nondegenerate squark masses would give rise to scalar couplings in most models [77]. However, there are still large regions of supersymmetric parameter space where the neutralino has primarily axial-vector interactions, and in fact, the Kane-Wells Higgsino candidate has primarily axial-vector interactions. The bottom line is that theory cannot currently reliably say which type of interaction the WIMP is likely to have, so experiments should continue to try to target both.

Cosmic Rays from WIMP Annihilation in the Galactic Halo: WIMPs may also be detected via observation of anomalous cosmic-ray positrons, antiprotons, and gamma rays produced by WIMP annihilation in the Galactic halo. The difficulty in inferring the existence of particle dark matter from cosmic rays lies in discrimination between WIMP-induced cosmic rays and those from standard “background” sources. However, WIMPs may produce distinctive cosmic-ray signatures. As illustrated in Fig. 12, WIMP annihilation will produce a cosmic-ray-positron excess at high energies that cannot be mimicked by any traditional astrophysical source. Similarly, WIMP annihilation will produce an antiproton excess at low energies that is difficult to explain with traditional astrophysical sources, as illustrated in Fig. 13. Direct annihilation of two WIMPs to two photons will produce a gamma-ray line at an energy equal to the WIMP mass. No other imaginable astrophysical mechanism could produce a monoenergetic gamma-ray signal at such an energy. It should be kept in mind, however, that due to several astrophysical uncertainties, it is difficult to make reliable predictions for a given particle dark-matter candidate, so negative results from cosmic-ray searches cannot generally be used to constrain dark-matter candidates. On the other hand, if observed, these cosmic-ray signatures could provide a smoking-gun signal for the existence of WIMPs in the halo.

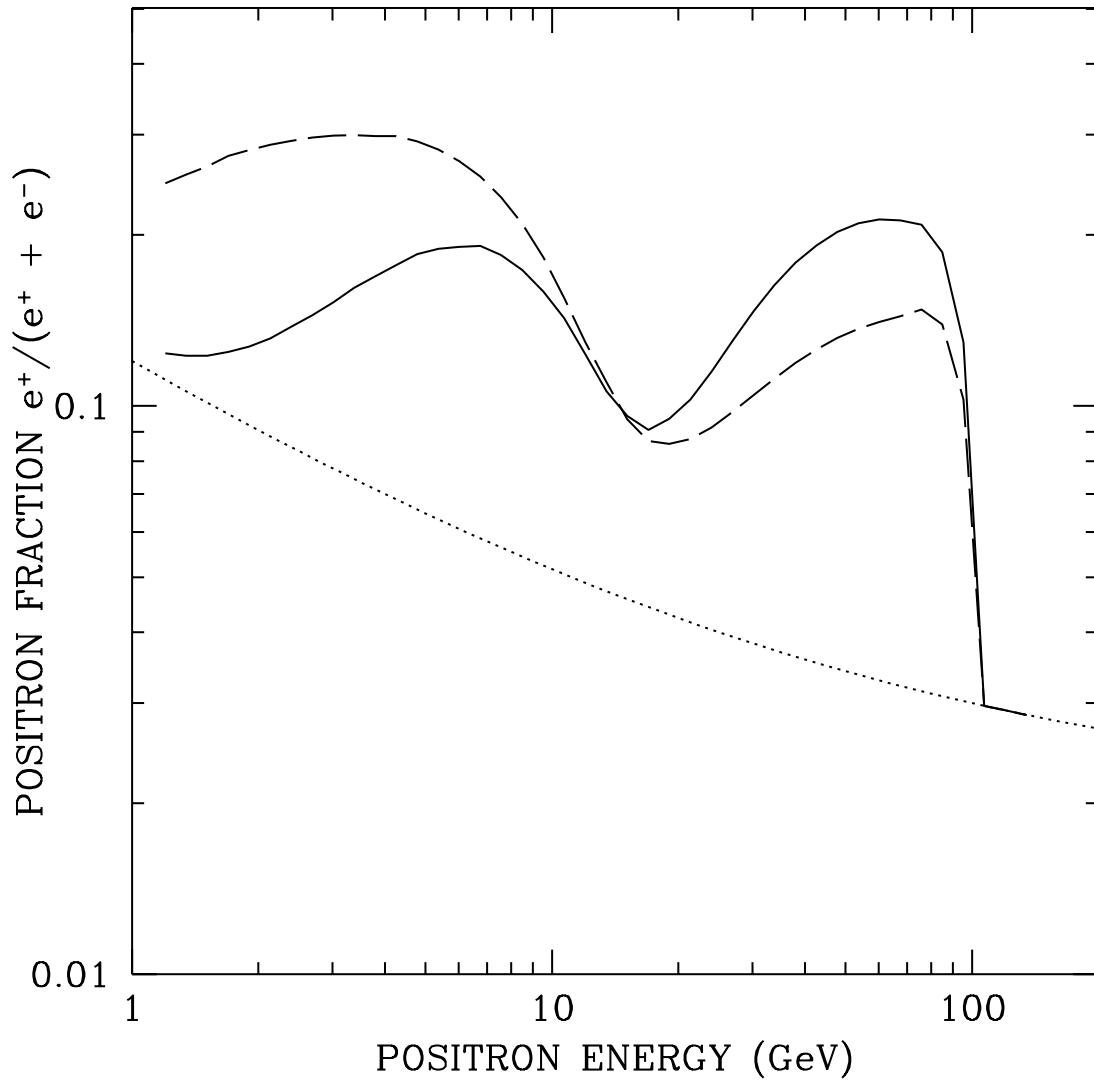


Figure 12: The differential positron flux divided by the sum of the differential electron-plus-positron flux as a function of energy for a neutralino of mass 120 GeV, for two different models of cosmic-ray propagation. The dotted curve is the background expected from traditional sources. From Ref. [78].

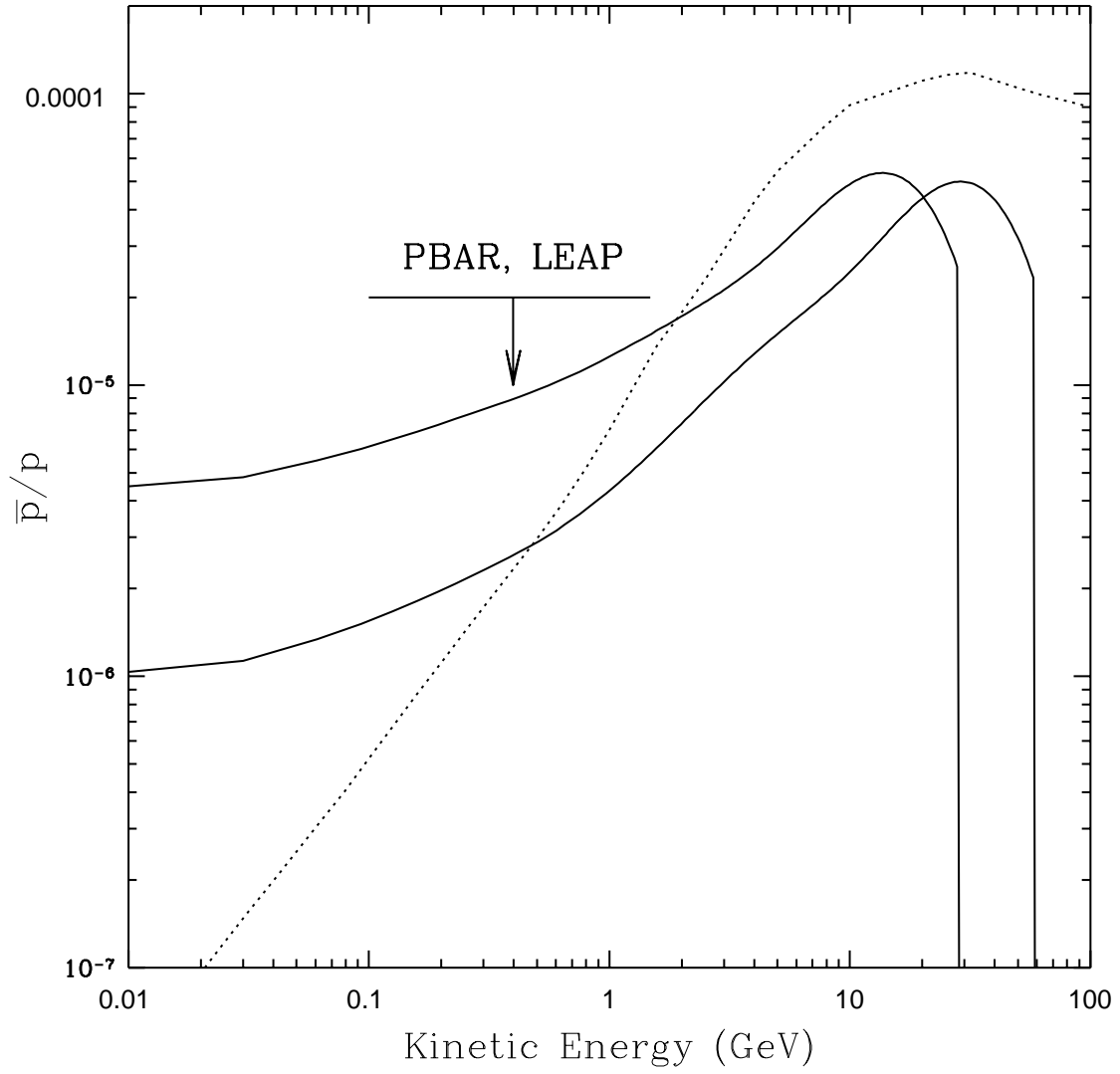


Figure 13: The differential cosmic-ray antiproton flux divided by the proton flux as a function of energy for a neutralino of mass 30 GeV and a neutralino of mass 60 GeV. The dotted curve is the background expected from traditional sources. Ref. [79].

4 Discussion

We are likely on the verge of great discoveries in cosmology. MAP and Planck will provide cosmological data of unprecedented precision that should clarify the origin of large-scale structure, and the values of several crucial cosmological parameters.

If MAP and Planck find a CMB temperature-anisotropy spectrum consistent with a flat Universe and nearly-scale-free primordial adiabatic perturbations, then the next step will be to isolate the gravity waves with the polarization of the CMB. If inflation has something to do with grand unification, then it is possible that Planck's polarization sensitivity will be sufficient to see the polarization signature of gravity waves. However, it is also quite plausible that the height of the inflaton potential may be low enough to elude detection by Planck. If so, then a subsequent experiment with better sensitivity to polarization will need to be done.

Since big-bang nucleosynthesis predicts that the baryon density is $\Omega_b \lesssim 0.1$ and inflation predicts $\Omega = 1$, another prediction of inflation is a significant component of nonbaryonic dark matter. This can be either in the form of vacuum energy (i.e., a cosmological constant), and/or some new elementary particle. Therefore, discovery of particle dark matter could be interpreted as evidence for inflation.

Axions and WIMPs have not only intrigued theorists; a large community of experimentalists have devoted themselves to finding these particles. However, it should also be emphasized that although very attractive, these are still speculative ideas. There is still no direct evidence in accelerator experiments or otherwise for the existence of axions or of supersymmetry. The dark matter could be composed of something completely different. However, as argued here, the evidence for the existence of nonbaryonic dark matter is indeed extremely compelling, and the two particles discussed here provide our most promising candidates. Although it provides an enormous experimental challenge, it is clear that discovery of particle dark matter would be truly revolutionary for both particle physics and cosmology.

Although most of the calculations needed for predicting rates for detection of supersymmetric dark matter have been completed and are amalgamated in Ref. [13], there continue to be new more general and/or more precise calculations. For example, just in the past year, there has been the first complete calculation of the cross section for neutralino annihilation to two photons [80] as well as the first calculation of the cross section for neutralino annihilation to a photon and a Z^0 boson, and these will be needed for accurate calculations of the strength of the photon line from WIMP annihilation in the Galactic halo. The possible effects of CP violation in the neutralino mass matrix have begun to be explored [82]. Some non-negligible three-body final states from neutralino annihilation have recently been discussed, and these may be important for accurate calculations of indirect-detection rates in certain regions of parameter space [83].

Before closing, it should be noted that there is even more that can be learned from the CMB and more ways to test and probe the physics of inflation. For example, inflation also predicts that the distribution of primordial density perturbations is gaussian, and this can be tested with CMB temperature maps and with the study of the large-scale distribution of galaxies.

As another example, large-scale galaxy surveys will soon map the distribution of mass in the Universe today, and CMB experiments will shortly determine the mass distribution in the early Universe. The next step will be to fill in the precise history of structure formation in the "dark ages" after recombination but before redshifts of a few. Reconstruction of this epoch of cosmic history will likely require amalgamation of the complementary information provided by a number observations in several wavebands. Detection of the secondary CMB anisotropies at arcminute scales produced by scattering from reionized clouds will provide an indication of the epoch of reionization, and therefore the epoch at which structures first undergo gravitational collapse in the Universe.

Acknowledgments

This work was supported by the U.S. D.O.E. Outstanding Junior Investigator Award under contract DEFG02-92-ER 40699, NASA NAG5-3091, and the Alfred P. Sloan Foundation.

References

1. A.H. Guth, *Phys. Rev. D* **28**, 347 (1981); A.D. Linde, *Phys. Lett. B* **108**, 389 (1982); A. Albrecht and P.J. Steinhardt, *Phys. Rev. Lett.* **48**, 1220 (1982).
2. J.M. Bardeen, P.J. Steinhardt, and M.S. Turner, *Phys. Rev. D* **28**, 679 (1983); A.A. Starobinsky, *Phys. Lett. B* **117**, 175 (1982); A.H. Guth and S.-Y. Pi, *Phys. Rev. Lett.* **49**, 1110 (1982); S.W. Hawking, *Phys. Lett. B* **115**, 295 (1982).
3. L.F. Abbott and M. Wise, *Nucl. Phys. B* **244**, 541 (1984).
4. A.R. Liddle and D. Lyth, *Phys. Lett. B* **291**, 391 (1992); R.L. Davis et al., *Phys. Rev. Lett.* **69**, 1856 (1992); M.S. Turner, *Phys. Rev. D* **48**, 3502 (1993); F. Lucchin, S. Matarrese, and S. Mollerach, *Astrophys. J. Lett.* **401**, L49 (1992); J.E. Lidsey and P. Coles, *Mon. Not. R. Astron. Soc.* **258**, L57 (1992); F.C. Adams et al., *Phys. Rev. D* **47**, 426 (1993); J. Lidsey et al., *Rev. Mod. Phys.* **69**, 373 (1997).
5. A.H. Jaffe, A. Stebbins, and J. Frieman, *Astrophys. J.* **420**, 9 (1994).
6. U.-L. Pen, U. Seljak, and N. Turok, *Phys. Rev. Lett.* **79**, 1611 (1997); A. Albrecht, R.A. Battye, and J. Robinson, *Phys. Rev. Lett.* **79**, 4736 (1997).
7. M. Kamionkowski, D.N. Spergel, and N. Sugiyama, *Astrophys. J. Lett.* **426**, L57 (1994).
8. K.G. Begeman, A.H. Broeils, and R.H. Sanders, *Mon. Not. R. Astr. Soc.* **249**, 523 (1991).
9. K.A. Olive, G. Steigman, D.N. Schramm, T.P. Walker, and H. Kang, *Astrophys. J.* **376**, 51 (1991).
10. S.D.M. White, C.S. Frenk, and M. Davis, *Astrophys. J.* **274**, L1-5 (1983).
11. S. Tremaine and J.E. Gunn, *Phys. Rev. Lett.*, **42**, 407 (1979).
12. For reviews, see, e.g., M.S. Turner, *Phys. Rep.* **197**, 67 (1990); G.G. Raffelt, *Phys. Rep.* **198**, 1 (1990). An illuminating pedagogical discussion has also been given recently by P. Sikivie, *Phys. Today* **49**, 22 (1996).
13. G. Jungman, M. Kamionkowski, and K. Griest, *Phys. Rep.* **267**, 195 (1996).
14. E.W. Kolb and M.S. Turner, *The Early Universe* (Addison-Wesley, Redwood City, 1989).
15. P.J.E. Peebles, *Principles of Physical Cosmology* (Princeton University Press, Princeton, 1993).
16. G.G. Raffelt, *Stars as Laboratories for Fundamental Physics* (University of Chicago Press, Chicago, 1996).
17. M. Kamionkowski, *Science* **280**, 1397 (1998).
18. C.H. Lineweaver and D. Barbosa, *Astrophys. J.* **496**, 624 (1998); S. Hancock et al., *Mon. Not. R. Astron. Soc.* **294**, L1 (1998).
19. <http://map.gsfc.nasa.gov>.
20. <http://astro.estec.esa.nl/SA-general/Projects/Planck/>
21. G. Jungman, M. Kamionkowski, A. Kosowsky, and D.N. Spergel, *Phys. Rev. Lett.* **76**, 1007 (1996).
22. G. Jungman, M. Kamionkowski, A. Kosowsky, and D.N. Spergel, *Phys. Rev. D* **54**, 1332 (1996).
23. J.R. Bond, G. Efstathiou, and M. Tegmark, *Mon. Not. R. Astron. Soc.* **291**, L33; M. Zaldarriaga, D.N. Spergel, and U. Seljak, *Astrophys. J.* **488**, 1 (1997).
24. W. Hu and M. White, *Phys. Rev. Lett.* **77**, 1687 (1996).
25. M. Kamionkowski, A. Kosowsky, and A. Stebbins, *Phys. Rev. Lett.* **78**, 2058 (1997).

26. M. Kamionkowski, A. Kosowsky, and A. Stebbins, *Phys. Rev. D* **55**, 7368 (1997).
27. U. Seljak and M. Zaldarriaga, *Phys. Rev. Lett.* **78**, 2054 (1997); M. Zaldarriaga and U. Seljak, *Phys. Rev. D* **55**, 1830 (1997).
28. M. Kamionkowski and A. Kosowsky, *Phys. Rev. D* **67**, 685 (1998).
29. W.H. Kinney, astro-ph/9806259.
30. M. Zaldarriaga, *Phys. Rev. D* **55**, 1822 (1997).
31. M. Tegmark, J. Silk, and A. Blanchard, *Astrophys. J.* **420**, 484 (1994).
32. Z. Haiman and A. Loeb, *Astrophys. J.* **483**, 21 (1997).
33. J.P. Ostriker and E.T. Vishniac, *Astrophys. J. Lett.* **306**, L51 (1986); E.T. Vishniac, *Astrophys. J.* **322**, 597 (1987); G. Efstathiou, in *Large-Scale Motions*, ed. V. Rubin and S.J. Coyne (Princeton University Press, Princeton, 1988); S. Dodelson and J.M. Jubas, *Astrophys. J.* **439**, 503 (1995); W. Hu, D. Scott, and J. Silk, *Phys. Rev. D* **49**, 648 (1994); W. Hu and M. White, *Astron. Astrophys.* **315**, 33 (1996).
34. A.H. Jaffe and M. Kamionkowski, *Phys. Rev. D* **58**, 043001 (1998).
35. M. White, J. Carlstrom, and M. Dragovan, astro-ph/9712195.
36. C. Athanassopoulos et al., *Phys. Rev. Lett.* **75**, 2650 (1995); *ibid*, *Phys. Rev. C* **54**, 2685 (1996).
37. J.R. Primack et al., *Phys. Rev. Lett.* **74**, 2160 (1995).
38. S. Dodelson, E. Gates, and A. Stebbins, *Astrophys. J.* **467**, 10 (1996).
39. W. Hu, D.J. Eisenstein, and M. Tegmark, *Phys. Rev. Lett.* **80**, 5255 (1998).
40. A.R. Liddle, A. Mazumdar, and J.D. Barrow, astro-ph/9802133.
41. X. Chen and M. Kamionkowski, work in progress.
42. L. A. Kofman and A. A. Starobinsky, *Sov. Astron. Lett.* **11**, 271 (1986).
43. R. G. Crittenden and N. G. Turok, *Phys. Rev. Lett.* **76**, 575 (1996).
44. M. Kamionkowski, *Phys. Rev. D* **54**, 4169 (1996).
45. S. P. Boughn, R. G. Crittenden, and N. G. Turok, *New Astronomy* **3**, 275 (1998).
46. M. Kamionkowski and A. Kinkhabwala, astro-ph/9808320.
47. R. Olling and D. Merrifield, astro-ph/9710224.
48. M. Kamionkowski and A. Kinkhabwala, *Phys. Rev. D* **57**, 3256 (1998).
49. R.D. Peccei and H.R. Quinn, *Phys. Rev. Lett.* **38**, 1440 (1977); F. Wilczek, *Phys. Rev. Lett.* **40**, 279 (1978); S. Weinberg, *Phys. Rev. Lett.* **40**, 223 (1978).
50. M.A. Bershadsky, M.T. Ressell, and M.S. Turner, *Phys. Rev. Lett.* **66**, 1398 (1991).
51. M. Kamionkowski and J. March-Russell, *Phys. Lett. B* **282**, 137 (1992); R. Holman et al., *Phys. Lett. B* **282**, 132 (1992); S. M. Barr and D. Seckel, *Phys. Rev. D* **46**, 539 (1992); B.A. Dobrescu, *Phys. Rev. D* **55**, 5826 (1997).
52. R. Holman et al., *Phys. Lett. B* **282**, 132 (1992); N. Turok, *Phys. Rev. Lett.* **76**, 1015 (1996); R. Kallosh et al., *Phys. Rev. D* **52**, 912 (1995); E.A. Dudas, *Phys. Lett. B* **325**, 124 (1994); K.S. Babu and S.M. Barr, *Phys. Lett. B* **300**, 367 (1993).
53. P. Sikivie, *Phys. Rev. Lett.* **51**, 1415 (1983).
54. K. van Bibber et al., *Int. J. Mod. Phys. Suppl. D* **3**, 33 (1994); C. Hagmann et al., *Nucl. Phys. (Proc. Suppl.) B* **51**, 209 (1996).
55. I. Ogawa, S. Matsuki, and K. Yamamoto, *Phys. Rev. D* **53**, 1740 (1996); S. Matsuki, I. Ogawa, and K. Yamamoto, *Phys. Lett. B* **336**, 573 (1994).
56. K. Griest and M. Kamionkowski, *Phys. Rev. Lett.* **64**, 615 (1990).
57. M. Beck, *Nucl. Phys. (Proc. Suppl.) B* **35**, 150 (1994); M. Beck et al., *Phys. Lett. B* **336**, 141 (1994); S.P. Ahlen et al., *Phys. Lett. B* **195**, 603 (1987); D.O. Caldwell et al., *Phys. Rev. Lett.* **61**, 510 (1988).
58. M. Mori et al. (Kamiokande Collaboration), *Phys. Lett. B* **289**, 463 (1992); M. Mori et al. (Kamiokande Collaboration), *Phys. Rev. D* **48**, 5505 (1993).
59. K. Griest and J. Silk, *Nature* **343**, 26 (1990); L.M. Krauss, *Phys. Rev. Lett.* **64**, 999

- (1990).
60. H.E. Haber and G.L. Kane, *Phys. Rep.* **117**, 75 (1985).
 61. T. Falk, K.A. Olive, and M. Srednicki, *Phys. Lett. B* **339**, 248 (1994).
 62. J. Ellis et al., *Nucl. Phys. B* **238**, 453 (1984); K. Griest, M. Kamionkowski, and M.S. Turner, *Phys. Rev. D* **41**, 3565 (1990).
 63. M.W. Goodman and E. Witten, *Phys. Rev. D* **31**, 3059 (1986); I. Wasserman, *Phys. Rev. D* **33**, 2071 (1986); K. Freese, J. Frieman, and A. Gould, *Phys. Rev. D* **37**, 3388 (1988); A. Drukier, K. Freese, and D.N. Spergel, *Phys. Rev. D* **33**, 3495 (1986).
 64. *J. Low Temp. Phys.* **93** (1993); P.F. Smith and J.D. Lewin, *Phys. Rep.* **187**, 203 (1990).
 65. P.D. Barnes et al., *J. Low Temp. Phys.* **93**, 79 (1993); T. Shutt et al., *Phys. Rev. Lett.* **61**, 3425 (1992); *ibid.*, 3531 (1992).
 66. J. Silk, K.A. Olive, and M. Srednicki, *Phys. Rev. Lett.* **55**, 257 (1985); K. Freese, *Phys. Lett. B* **167**, 295 (1986); L.M. Krauss, K. Freese, D.N. Spergel, and W.H. Press, *Astrophys. J.* **299**, 1001 (1985); L.M. Krauss, M. Srednicki, and F. Wilczek, *Phys. Rev. D* **33**, 2079 (1986); T. Gaisser, G. Steigman, and S. Tilav, *Phys. Rev. D* **34**, 2206 (1986); M. Kamionkowski, *Phys. Rev. D* **44**, 3021 (1991); S. Ritz and D. Seckel, *Nucl. Phys. B* **304**, 877 (1988); F. Halzen, M. Kamionkowski, and T. Stelzer, *Phys. Rev. D* **45**, 4439 (1992).
 67. J.M. LoSecco et al. (IMB Collaboration), *Phys. Lett. B* **188**, 388 (1987).
 68. M.M. Boliev et al., *Bull. Acad. Sci. USSR, Phys. Ser.* **55**, 126 (1991) [*Izv. Akad. Nauk. SSSR, Fiz.* **55**, 748 (1991)]; M.M. Boliev et al., in *TAUP 95*, proceedings of the Workshop, Toledo, Spain, September 17–21, 1995, ed. A. Morales, J. Morales and J.A. Villar, [*Nucl. Phys. (Proc. Suppl.) B* **48**, 83 (1996)] (North-Holland, Amsterdam, 1996).
 69. L. Bergstrom, J. Edsjö, and M. Kamionkowski, *Astropart. Phys.* **7**, 147 (1997).
 70. Y. Ho (HANUL Collaboration), to appear in *Very High Energy Phenomena in the Universe*, proceedings of the XXXIIInd Moriond Conference, ed. J. Tran Thanh Van (Editions Frontières, Gif-sur-Yvette, 1997).
 71. J. Rich and C. Tao, DAPNIA/SPP 95-01.
 72. M. Kamionkowski, K. Griest, G. Jungman, and B. Sadoulet, *Phys. Rev. Lett.* **74**, 5174 (1995).
 73. G.L. Kane and J.D. Wells, *Phys. Rev. Lett.* **76**, 4458 (1996); S. Ambrosanio et al., *Phys. Rev. Lett.* **76**, 3498 (1996).
 74. S. Park, “Search for New Phenomena at CDF,” 10th Topical Workshop on Proton-Antiproton Collider Physics, edited by R. Raja and J. Yoh (AIP Press, 1996).
 75. K. Freese and M. Kamionkowski, *Phys. Rev. D* **55**, 1771 (1997).
 76. K. Griest, *Phys. Rev. D* **38**, 2357 (1988); FERMILAB-Pub-89/139-A (E).
 77. M. Drees and M.M. Nojiri, *Phys. Rev. D* **47**, 4226 (1993); *ibid.* **48**, 3483 (1993).
 78. M. Kamionkowski and M.S. Turner, *Phys. Rev. D* **43**, 1774 (1991).
 79. G. Jungman and M. Kamionkowski, *Phys. Rev. D* **49**, 2316 (1994).
 80. L. Bergstrom and P. Ullio, *Nucl. Phys. B* **504**, 27 (1997).
 81. P. Ullio and L. Bergstrom, *Phys. Rev. D* **57**, 1962 (1998).
 82. T. Falk, A. Ferstl, and K. A. Olive, hep-ph/9806413.
 83. X. Chen and M. Kamionkowski, *J. High Energy Phys.* 07(1998)001.